

R-Parity Violating Supersymmetry and the 125 GeV Higgs signals

Jonathan Cohen,^{1,*} Shaouly Bar-Shalom,^{1,†} Gad Eilam,^{1,‡} and Amarjit Soni^{2,§}

¹*Physics Department, Technion–Institute of Technology, Haifa 3200003, Israel*

²*Physics Department, Brookhaven National Laboratory, Upton, NY 11973, US*

(Dated: October 1, 2019)

We study the impact of R-parity violating Supersymmetry (RPV SUSY) on the 125 GeV Higgs production and decay modes at the LHC. We assume a heavy SUSY spectrum with multi-TeV squarks and SU(2) scalar singlets as well as the decoupling limit in the SUSY Higgs sector. In this case the lightest CP-even Higgs is SM-like when R-parity is conserved. In contrast, we show that when R-parity violating interactions are added to the SUSY framework, significant deviations may occur in some production and decay channels of the 125 GeV Higgs-like state. Indeed, we assume a single-flavor (mostly third generation) Bilinear RPV (BRPV) interactions, which generate Higgs-sneutrino mixing, lepton-chargino mixing and neutrino-neutralino mixing, and find that notable deviations of $\mathcal{O}(20-30\%)$ may be expected in the Higgs signal strength observables in some channels, e.g., in $pp \rightarrow h \rightarrow \mu^+ \mu^-, \tau^+ \tau^-$. Moreover, we find that new and detectable signals associated with BRPV Higgs decays to gauginos, $h \rightarrow \nu_\tau \tilde{\chi}_2^0$ and $h \rightarrow \tau^\pm \tilde{\chi}_2^\mp$, may also arise in this scenario. These decays yield a typical signature of $h \rightarrow \tau^\pm \ell^\mp + \cancel{E}_T$ ($\ell = e, \mu, \tau$) that can be much larger than in the SM, and may also be accompanied by an $\mathcal{O}(20-30\%)$ enhancement in the di-photon signal $pp \rightarrow h \rightarrow \gamma\gamma$. We also examine potential interesting signals of Trilinear R-parity violation (TRPV) interactions in the production and decays of the Higgs-sneutrino BRPV mixed state (assuming it is the 125 GeV scalar) and show that, in this case also, large deviations up to $\mathcal{O}(100\%)$ are expected in e.g., $pp \rightarrow h \rightarrow \mu^+ \mu^-, \tau^+ \tau^-$, which are sensitive to the BRPV \times TRPV coupling product.

I. INTRODUCTION

The discovery of the 125 GeV Higgs boson in 2012 [1, 2] has marked the starting point of a new era in particle physics, that of Higgs precision measurements, thus leading to a joint effort by both theorists and experimentalists, in order to unravel the true nature of the Higgs and its possible connection to New Physics (NP) beyond the SM (BSM).

The ATLAS and CMS experiments have made since then outstanding progress in the measurements of the various Higgs production and decay modes, which serve as an important testing ground of the SM. Indeed, the current status is that the measured Higgs signals are largely compatible with the SM within the errors; in some channels the combined precision is of $\mathcal{O}(10\%)$ at the 1σ level [3–14]. In particular, in the SM the main Higgs production modes include the dominant gluon-fusion channel (predominantly through the top-quark loop), $gg \rightarrow h$, as well as the hV and Vector-Boson-Fusion (VBF) channels, $q\bar{q} \rightarrow V \rightarrow hV$ and $VV \rightarrow h$ (the overall hard process being $qq \rightarrow qqh$), respectively. Its dominant decay mode is $h \rightarrow b\bar{b}$, which is currently measured only via the sub-dominant hV production mode (due to the large QCD background in the leading model $gg \rightarrow h \rightarrow b\bar{b}$). The best sensitivity, at the level of $\mathcal{O}(10\%)$ (combining the ATLAS and CMS measurements [5–10]) is currently obtained in the Higgs decay channels to vector-bosons $h \rightarrow \gamma\gamma, ZZ^*, WW^*$, when it is produced in the gluon-fusion channel.

Thus, by looking for patterns of deviations in the Higgs properties, these so-called "Higgs-signals" can, therefore, shed light on the UV theory which underlies the SM. Indeed, the Higgs plays an important role in many of the popular BSM scenarios that attempt to address the fundamental shortcomings of the SM, such as the hierarchy and flavor problems, dark matter and neutrino masses. For that reason Higgs physics has been studied within several well motivated BSM scenarios such as supersymmetry (SUSY) [15–17], which addresses the hierarchy problem and Composite Higgs-models [18], in which the Higgs is identified as a pseudo-Nambu-Goldstone boson associated with the breaking of an underlying global symmetry. The Higgs has also been extensively studied in a model-independent approach, using the so called SMEFT framework [19], where it is incorporated in higher dimensional operators and in Higgs-portal models [20–24], which address the dark matter problem.

It is widely accepted that perhaps the most appealing BSM theoretical concept is SUSY, since it essentially eliminates the gauge hierarchy problem (leaving perhaps a little hierarchy in the SUSY fundamental parameter space) and it elegantly addresses the unification of forces, as well as providing a well motivated dark matter candidate. Unfortunately, no SUSY particles have yet been observed, so that the typical SUSY scale is now pushed to the multi-TeV

* jcohen@campus.technion.ac.il

† shaouly@physics.technion.ac.il

‡ eilam@physics.technion.ac.il

§ adlersoni@gmail.com

range, with the exception of some of the Electro-Weak (EW) interacting SUSY states, such as the lightest gauginos and SU(2) sleptons doublets. An interesting variation of SUSY, which is in fact a more general SUSY framework, includes R-parity violating (RPV) interactions [25]. Indeed, one of the key incentives of the the RPV SUSY framework is the fact that it also addresses the generation of neutrino masses in a distinctive manner. Many studies on RPV SUSY have, therefore, focused on reconstructing the neutrino masses and oscillation data [26–41], while far less attention has been devoted to the role that RPV SUSY may play in Higgs Physics [42–53]. It has also been recently proposed, that an effective RPV SUSY scenario approach involving only the third generation [54] can simultaneously explain the $R_{D^{(*)}}$ anomaly related to B-physics and also alleviate the Hierarchy problem of the SM [55]. For related efforts tackling the recent B-anomalies within the RPV SUSY framework see [56–58].

From the experimental side, since RPV entails the decay of the LSP, the searches for RPV signatures at the LHC are based on a different strategy than in traditional SUSY channels [59–66].

In this paper, we propose to interpret the observed 125 GeV Higgs-like state as a Higgs-sneutrino mixed state of the RPV SUSY framework [67, 68] (throughout the paper we will loosely refer to the Higgs-sneutrino mixed state as the "Higgs"). We thus study the implications and effects of RPV SUSY on the 125 GeV Higgs signals. Guided by the current non-observation of SUSY particles at the LHC, we adopt a heavy SUSY spectrum with multi-TeV squarks and SU(2) scalar singlets as well as the decoupling limit in the SUSY Higgs sector. We find that, in contrast to the R-parity conserving (RPC) heavy SUSY scenario, where the lightest CP-even Higgs is SM-like, the RPV interactions can generate appreciable deviations from the SM rates in some production and decay channels of the lightest 125 GeV Higgs-sneutrino mixed state. These are generated by either Bilinear RPV (BRPV) interactions or BRPV combined with Trilinear RPV (TRPV) interactions. In particular, we find that notable effects ranging from $\mathcal{O}(20 - 30\%)$ up to $\mathcal{O}(100\%)$ may be expected in the Higgs signal strength observables in the channels, $pp \rightarrow h \rightarrow \mu^+\mu^-, \tau^+\tau^-$ and in the di-photon signal $pp \rightarrow h \rightarrow \gamma\gamma$ and that new sizable signals (see eq. (34)) associated with BRPV Higgs decays to gauginos, $h \rightarrow \tau^\pm \ell^\mp + \cancel{E}_T$ ($\ell = e, \mu, \tau$), may also occur in this scenario. We study these Higgs production and decay channels under all the available constraints on the RPV SUSY parameter space.

The paper is organized as follows: in section II we briefly describe the RPV SUSY framework and in section III we layout our notation and give an overview of the measured signals of the 125 GeV Higgs-like state. In sections IV and V we present our analysis and results for the BRPV and TRPV Higgs signals, respectively, and in section VI we summarize. In Appendix A we give the relevant RPV Higgs couplings, decays and production channels, while in Appendix B we list the SUSY spectra associated with the RPV SUSY benchmark models studied in the paper.

II. THE RPV SUSY FRAMEWORK

The SUSY RPC superpotential is (see e.g., [15–17, 69]):

$$\mathcal{W}_{\text{RPC}} = \epsilon_{ab} \left[\frac{1}{2} h_{jk} \hat{H}_d \hat{L}_j \hat{E}_k + h'_{jk} \hat{H}_d \hat{Q}_j \hat{D}_k + h''_{jk} \hat{H}_u \hat{Q}_j \hat{U}_k - \mu \hat{H}_d \hat{H}_u \right], \quad (1)$$

where \hat{H}_u (\hat{H}_d) are the up(down)-type Higgs supermultiplet and \hat{L} (\hat{E}^c) are the leptonic SU(2) doublet(charged singlet) supermultiplets. The \hat{Q} are quark SU(2) doublet supermultiplets and \hat{U}^c (\hat{D}^c) are SU(2) up(down)-type quark singlet supermultiplets. Also, $j, k = 1, 2, 3$ are generation labels and SU(2) contractions are not explicitly shown.

If R-parity is violated, then both lepton and baryon numbers may no longer be conserved in the theory. In particular, when lepton number is violated then the \hat{L} and \hat{H}_d superfields, which have the same gauge quantum numbers, lose their identity since there is no additional quantum number that distinguishes between them. One can then construct additional renormalizable RPV interactions simply by replacing $\hat{H}_d \rightarrow \hat{L}$ in (1). Thus, the SUSY superpotential can violate lepton number (or more generally R-parity) via Yukawa-like trilinear term (TRPV) and/or a mass-like bilinear RPV term (BRPV) as follows (see e.g., [25, 70–75]):

$$\mathcal{W}_{\text{RPV}(\cancel{R})} \supset \frac{1}{2} \lambda_{ijk} \hat{L}_i \hat{L}_j \hat{E}_k + \lambda'_{ijk} \hat{L}_i \hat{Q}_j \hat{D}_k - \epsilon_i \hat{L}_i \hat{H}_u. \quad (2)$$

where λ_{ijk} is anti-symmetric in the first two indices $i \neq j$ due to SU(2) gauge invariance (here also SU(2) labels are not shown).

Moreover, if R-parity is not conserved then, in addition to the usual RPC soft SUSY breaking terms, one must also add new trilinear and bilinear soft terms corresponding to the RPV terms of the superpotential, e.g., to the ones in (2). For our purpose, the relevant ones to be added to the SUSY scalar potential are the following soft breaking mass-like terms [26, 30, 32, 76–80]:

$$V_{BRPV} = (M_{\tilde{L}H}^2)_i \tilde{L}_i H_d - (B_\epsilon)_i \tilde{L}_i H_u , \quad (3)$$

where \tilde{L} and H_d are the scalar components of \hat{L} and \hat{H}_d , respectively.

In what follows, we will consider a single generation BRPV scenario, i.e., that in eq. (3) R-Parity is violated only among the interactions of a single slepton. In particular, we will be focusing mainly on the 3rd generation bilinear soft breaking mixing term, $(B_\epsilon)_3$, which mixes the 3rd generation (tau-flavored) left-handed slepton neutral and charged fields with the neutral and charged up-type Higgs fields, respectively. The bilinear soft term $(B_\epsilon)_3$ leads in general to a non-vanishing VEV of the tau-sneutrino, $\langle \tilde{\nu}_\tau \rangle = v_{\tilde{\nu}_\tau}$. However, since lepton number is not a conserved quantum number in this scenario, the \hat{H}_d and \hat{L}_3 superfields lose their identity and can be rotated to a particular basis (\hat{H}'_d, \hat{L}'_3) in which either ϵ_3 or $v_3 = v_{\tilde{\nu}_\tau}$ are set to zero [26, 80–83]. In what follows, we choose for convenience to work in the \hat{L} no VEV basis, $v_{\tilde{\nu}_\tau} = 0$, which simplifies our analysis below. In this basis the minima conditions in the scalar potential read (we follow below the notation of the package SARAH [84–86] and use some of the expressions given in [87]):

$$1) \quad m_{H_d}^2 v_d - v_u B_\mu + \frac{1}{8} (g_1^2 + g_2^2) v_d (-v_u^2 + v_d^2) + |\mu|^2 v_d = 0 , \quad (4)$$

$$2) \quad -\frac{1}{8} (g_1^2 + g_2^2) v_u (-v_u^2 + v_d^2) + \frac{1}{2} \left(-2v_d B_\mu + 2v_u \left(m_{H_u}^2 + |\mu|^2 + |\epsilon_3|^2 \right) \right) = 0 , \quad (5)$$

$$3) \quad (m_{LH}^2)_3 + (B_\epsilon)_3 \tan \beta - \epsilon_3 \mu = 0 , \quad (6)$$

where B_μ is the soft breaking bilinear term $B_\mu H_d H_u$ (i.e., corresponding to the μ -term in the superpotential) and v_u, v_d are the VEV's of the up and down Higgs fields, H_u^0, H_d^0 .

Without loss of generality, in what follows, we parameterize B_μ in terms of the physical pseudo-scalar mass m_A using the RPC MSSM relation $m_A^2 \equiv \csc \beta \sec \beta B_\mu$ (see e.g., [44]), thus defining the soft BRPV "measure" as (from now on and throughout the rest of the paper we drop the generation index of the BRPV terms):

$$\delta_B \equiv \frac{B_\epsilon}{B_\mu} , \quad (7)$$

so that B_ϵ will be given in terms of a new BRPV parameter δ_B :

$$B_\epsilon \equiv \delta_B B_\mu = \frac{1}{2} m_A^2 \sin(2\beta) \delta_B . \quad (8)$$

We also define, in a similar way, the measure of BRPV in the superpotential, δ_ϵ , via:

$$\epsilon \equiv \delta_\epsilon \mu . \quad (9)$$

A. The RPV SUSY scalar sector and Higgs-Sneutrino mixing

Using eqs. (4)–(8), the induced CP-odd and CP-even scalar mass matrices squared reads (see e.g., [87]):^{1,2}

$$m_O^2 = \begin{pmatrix} s_\beta^2 m_A^2 & m_A^2 s_\beta c_\beta & -\delta_B m_A^2 s_\beta^2 \\ m_A^2 s_\beta c_\beta & c_\beta^2 m_A^2 & -\delta_B m_A^2 s_\beta c_\beta \\ -\delta_B m_A^2 s_\beta^2 & -\delta_B m_A^2 s_\beta c_\beta & m_{\tilde{\nu}_\tau}^2 \end{pmatrix} \quad (10)$$

$$m_E^2 = \begin{pmatrix} s_\beta^2 m_A^2 + m_Z^2 c_\beta^2 + \delta_{11}^{t-i} & -s_\beta c_\beta m_A^2 - m_Z^2 s_\beta c_\beta + \delta_{12}^{t-i} & -\delta_B m_A^2 s_\beta^2 \\ -s_\beta c_\beta m_A^2 - m_Z^2 s_\beta c_\beta + \delta_{12}^{t-i} & c_\beta^2 m_A^2 + m_Z^2 s_\beta^2 + \delta_{22}^{t-i} & \delta_B m_A^2 s_{2\beta}/2 \\ -\delta_B m_A^2 s_\beta^2 & \delta_B m_A^2 s_{2\beta}/2 & m_{\tilde{\nu}_\tau}^2 \end{pmatrix} \quad (11)$$

¹ The CP-odd scalar mass matrix, m_O^2 , has a massless state which corresponds to the Goldstone boson.

² We note that too large values of δ_B may drive (depending on the other free-parameters in the Higgs sector) the lightest mass-squared eigenstates of both the CP-even and CP-odd mass matrices to non-physical negative values. We will thus demand non-negative mass-squared physical eigenvalues for the CP-even and CP-odd physical states by bounding δ_B accordingly.

with $s_\beta \equiv \sin \beta$, $c_\beta \equiv \cos \beta$ and $\tan \beta = v_u/v_d$. The τ -sneutrino mass term, $m_{\tilde{\nu}_\tau}$, is given in the RPV SUSY framework by:

$$m_{\tilde{\nu}_\tau}^2 = \underbrace{m_{\tilde{\tau}_{LL}}^2 + \frac{1}{8} (g_1^2 + g_2^2) (-v_u^2 + v_d^2)}_{(m_{\tilde{\nu}_\tau}^2)_{RPC}} + |\epsilon|^2, \quad (12)$$

where $m_{\tilde{\tau}_{LL}}$ is the soft left-handed slepton mass term, $m_{\tilde{\tau}_{LL}}^2 \tilde{L}_3^* \tilde{L}_3$. We have denoted in eq. (12) the τ -sneutrino mass term in the RPC limit $\epsilon \rightarrow 0$ by $(m_{\tilde{\nu}_\tau}^2)_{RPC}$ (note that the correction to $m_{\tilde{\nu}_\tau}^2$ in the BRPV framework is $(\Delta m_{\tilde{\nu}_\tau}^2)_{RPV} = |\epsilon|^2$). Note also that we have added in the CP-even sector the dominant top-stop loop corrections, $\delta_{ij}^{t-\tilde{t}}$, which are required in order to lift the lightest Higgs mass to its currently measured value [88]; see also discussion on the Higgs mass filter in section IV.

The physical CP-even mass eigenstates in the RPV framework, which we denote below by $S_{RPV}^E = (h_{RPV}, H_{RPV}, \tilde{\nu}_{RPV})^T$, are obtained upon diagonalizing the CP-even scalar mass-squared matrix:

$$S^E = Z^E S_{RPV}^E, \quad (13)$$

where $S^E = (H_d, H_u, \tilde{\nu}_\tau)^T$ are the corresponding weak states of in the CP-even Higgs sector and Z_E is the unitary 3×3 matrix which diagonalizes m_E^2 , defined here as:

$$Z^E = \begin{pmatrix} Z_{h1} & Z_{H1} & Z_{\tilde{\nu}1} \\ Z_{h2} & Z_{H2} & Z_{\tilde{\nu}2} \\ Z_{h3} & Z_{H3} & Z_{\tilde{\nu}3} \end{pmatrix}. \quad (14)$$

We would like to emphasize a few aspects and features of the BRPV SUSY framework which are manifest in the CP-even Higgs mass matrix and spectrum and are of considerable importance for our study in this paper:

- We will be interested in the properties (i.e., production and decay modes) of h_{RPV} , which is the lightest CP-even Higgs state in the BRPV framework. This state has a Sneutrino component due to the Higgs-sneutrino mixing terms (i.e., $\propto \delta_B$) in the CP-even Higgs mass matrix [67, 68]. The element Z_{h3} is the one which corresponds to the Sneutrino component in h_{RPV} and is, therefore, responsible for the $\tilde{\nu}_\tau - h$ mixing phenomena. It depends on δ_B and thus shifts some of the RPC light-Higgs couplings, as will be discussed below. In particular, we interpret the observed 125 GeV Higgs-like state as the lightest Higgs-sneutrino mixed state h_{RPV} and, in our numerical simulations below, we demand $122 < m_{h_{RPV}} < 128$ GeV, in accordance with the LHC data where we allow some room for other SUSY contributions to the Higgs mass, i.e., beyond the simplified RPV framework discussed in this work.
- The elements Z_{h1} and Z_{h2} correspond to the H_d^0 and H_u^0 components in h_{RPV} . They are independent of the soft BRPV parameter δ_B at $\mathcal{O}(\delta_B)$, so that, at leading order in δ_B , they are the same as the corresponding RPC elements.
- Guided by the current non-observation of new sub-TeV heavy Higgs states at the LHC, we will assume the decoupling limit in the SUSY Higgs sector [17, 89, 90], in which case the RPC Higgs couplings are SM-like. We will demonstrate below that the BRPV effects may be better disentangled in this case.

B. The Gaugino sector

With the BRPV term in the superpotential ($\epsilon \hat{L} \hat{H}_u$ in eq. (2)) and assuming only 3rd generation BRPV, i.e., only $\epsilon_3 \neq 0$, the neutralinos and charginos mass matrices read:

$$m_N = \begin{pmatrix} (m_{\nu_\tau})_{loop}^{\delta_B \delta_B} + (m_{\nu_\tau})_{loop}^{\delta_B \delta_\epsilon} & V_N^{BRPV} \\ (V_N^{BRPV})^T & m_N^{RPC} \end{pmatrix}, \quad (15)$$

$$m_C = \begin{pmatrix} m_\tau & V_C^{BRPV} \\ \vec{0}^T & m_C^{RPC} \end{pmatrix}, \quad (16)$$

where $V_N^{BRPV} \equiv (0, 0, 0, \delta_\epsilon \mu)$, $V_C^{BRPV} \equiv (0, -\delta_\epsilon \mu)$, $\vec{0} = (0, 0)$ and $\delta_\epsilon = \epsilon/\mu$ (dropping the generation index, see eq. (9)). Also, $(m_C)_{11} = m_\tau$ is the bare mass of the τ -lepton and in $(m_N)_{11}$ we have added the loop-induced BRPV contributions $(m_{\nu_\tau})_{loop}^{\delta_B \delta_B}$ and $(m_{\nu_\tau})_{loop}^{\delta_B \delta_\epsilon}$ to the tau-neutrino mass [34] (which is used in section IV in order to constrain the BRPV parameters δ_B and δ_ϵ). Finally, $m_N^{RPC} = m_N^{RPC}(M_1, M_2, \mu, m_Z, \tan \beta, s_W)$ and $m_C^{RPC} = m_C^{RPC}(M_2, \mu, m_Z, \tan \beta, s_W)$ are the 4×4 neutralino mass matrix and the 2×2 chargino mass matrix in the RPC limit, respectively, which depend on the U(1) and SU(2) gaugino mass terms M_1 and M_2 , on the bilinear RPC μ term, on $\tan \beta$ and on the Z-boson mass m_Z and the Weinberg angle θ_W (see e.g., [87]).

The physical neutralino and chargino states, $F_{RPV}^{\tilde{\chi}^0} = (\tilde{\chi}_1^0, \tilde{\chi}_2^0, \tilde{\chi}_3^0, \tilde{\chi}_4^0, \tilde{\chi}_5^0)^T$ and $F_{RPV}^{\chi^\pm} = (\chi_1^\pm, \chi_2^\pm, \chi_3^\pm)^T$, respectively, are obtained by diagonalizing their mass matrices in (15) and (16). For the neutralinos we have (i.e., with only 3rd generation neutrino-neutralino mixing):

$$F^{\tilde{\chi}^0} = U_N F_{RPV}^{\tilde{\chi}^0}, \quad (17)$$

where $F^{\tilde{\chi}^0} = (\nu_\tau, \tilde{B}, \tilde{W}, \tilde{H}_d, \tilde{H}_u)^T$ are the neutralino weak states and U_N is the unitary matrix which diagonalizes m_N in (15). In particular, we identify the lightest neutralino state in the RPV setup, $\tilde{\chi}_1^0$, as the τ -neutrino $\tilde{\chi}_1^0 \equiv \nu_\tau$. Note that the entries $(U_N)_{ij}$ enter in the Higgs couplings to a pair of neutralinos and, in particular, generates the coupling $h\nu_\tau \tilde{\chi}_2^0$ ($h \equiv h_{RPV}$), where $\tilde{\chi}_2^0$ is the 2nd lightest neutralino state corresponding to the lightest neutralino in the RPC case (see Appendix A 4). As will be discussed in section IV, this new RPV coupling opens a new Higgs decay channel $h \rightarrow \nu_\tau \tilde{\chi}_2^0$, if $m_{\tilde{\chi}_2^0} < m_h$ and also enters in the the loop-induced contribution to m_{ν_τ} .

In the chargino's case, since the matrix m_C is not symmetric, it is diagonalized with the singular value decomposition procedure, which ensures a positive mass spectrum:

$$U_L m_C U_R^\dagger = m_C^{diag}. \quad (18)$$

The chargino physical states (χ_i^\pm) are then obtained from the weak states $F^{\chi^-} = (\tau_L, \tilde{W}^-, \tilde{H}_d^-)^T$ and $F^{\chi^+} = (\tau_R, \tilde{W}^+, \tilde{H}_u^+)^T$ by:

$$F^{\chi^-} = (U_L)^T F_{RPV}^{\chi^-}, \quad F^{\chi^+} = U_R F_{RPV}^{\chi^+}, \quad (19)$$

where, here also, the lightest chargino is identified as the τ -lepton, i.e., $\tau^+ = \chi_1^+$ and the elements of the chargino rotation matrices $U_{L,R}$ enter in the Higgs couplings to a pair of charginos. Thus, the decay $h \rightarrow \chi_1^+ \chi_1^-$ corresponds in the RPV framework to $h \rightarrow \tau^+ \tau^-$. In addition, if $m_\tau + m_{\chi_2^+} < m_h$, then the decay $h \rightarrow \tau^\pm \chi_2^\mp$ (i.e., the decay $h \rightarrow \chi_1^\pm \chi_2^\mp$) is also kinematically open (see Appendix A 4).

III. THE 125 GEV HIGGS SIGNALS

The measured signals of the 125 GeV Higgs-like particle are sensitive to a variety of new physics scenarios, which may alter the Higgs couplings to the known SM particles that are involved in its production and decay channels.

We will use below the Higgs "signal strength" parameters, which are defined as the ratio between the Higgs production and decay rates and their SM expectations:

$$\mu_{if}^{(P)} \equiv \mu_i^{(P)} \cdot \mu_f \cdot \frac{\Gamma_{SM}^h}{\Gamma_h}, \quad (20)$$

where $\mu_i^{(P)}$ and μ_f are the normalized production and decays factors which, in the narrow Higgs width approximation, read:

$$\mu_i^{(P)} = \frac{\sigma(i \rightarrow h)}{\sigma(i \rightarrow h)_{SM}}, \quad \mu_f = \frac{\Gamma(h \rightarrow f)}{\Gamma(h \rightarrow f)_{SM}}, \quad (21)$$

and Γ^h (Γ_{SM}^h) is the total width of the 125 GeV Higgs (SM Higgs). Also, i represents the parton content in the proton which is involved in the production mechanism and f is the Higgs decay final state.

We will consider below the signal strength signals which are associated with the leading hard production mechanisms:

TABLE I: Combined ATLAS and CMS (13 TeV) signal strength measurements corresponding to the Higgs observables defined in eq. (20). We have closely followed the Higgs data as summarized in Table I in [92], with some updated more recent results where needed (citations to the relevant papers are given in the 3rd column). Note that we have added the recent combined signal strength measurement in the $pp \rightarrow h \rightarrow \mu\mu$ channel, $\mu_F^{(gg)}$. Also, in each channel, we have indicated (with a superscript) the specific hard production channel (gg , hV or VBF), see also text.

ATLAS + CMS		
$\mu_{Vbb}^{(hV/hW)}$	$1.07^{+0.23}_{-0.22}$	[3, 4]
$\mu_{Vbb}^{(hZ)}$	$1.20^{+0.33}_{-0.31}$	[3]
$\mu_{FWW}^{(gg)}$	$1.24^{+0.15}_{-0.16}$	[5, 6]
$\mu_{FZZ}^{(gg)}$	$1.09^{+0.11}_{-0.11}$	[7, 8]
$\mu_{F\gamma\gamma}^{(gg)}$	$1.02^{+0.12}_{-0.11}$	[9, 10]
$\mu_{F\tau\tau}^{(gg)}$	$1.06^{+0.40}_{-0.37}$	[11, 12]
$\mu_{V\gamma\gamma}^{(VBF)}$	$1.10^{+0.36}_{-0.31}$	[9, 10]
$\mu_{V\tau\tau}^{(VBF)}$	$1.15^{+0.36}_{-0.34}$	[11, 12]
$\mu_{F\mu\mu}^{(gg)}$	$0.55^{+0.70}_{-0.70}$	[13, 14]

gluon-fusion, $gg \rightarrow h$, hV production, $q\bar{q} \rightarrow V \rightarrow hV$, and VBF, $VV \rightarrow h$.³ The $q\bar{q}$ -fusion production channel, which is negligible in the SM due to the vanishingly small SM Yukawa couplings of the light-quarks, will be considered for the TRPV scenario in the next section. We will use the usual convention, denoting by $i = F$ the gluon-fusion channel and by $i = V$ the hV and VBF channels; for clarity and consistency with the above definitions, we will also explicitly denote the underlying hard production mechanism by a bracketed superscript. The decay channels that will be considered below are $h \rightarrow \gamma\gamma$, WW^* , ZZ^* and $h \rightarrow \mu^+\mu^-$, $\tau^+\tau^-$, $b\bar{b}$.

In particular, in the BRPV SUSY scenario we have:

$$\mu_F^{(gg)} = \frac{\Gamma(h \rightarrow gg)}{\Gamma(h \rightarrow gg)_{SM}}, \quad (22)$$

$$\mu_V^{(hV)} = \mu_V^{(VBF)} = (g_{hVV}^{RPC})^2, \quad (23)$$

for the production factors and

$$\mu_{bb} = (g_{hbb}^{RPC})^2, \quad (24)$$

$$\mu_{VV^*} = (g_{hVV}^{RPC})^2, \quad (25)$$

$$\mu_{\mu\mu/\tau\tau} = \frac{\Gamma(h \rightarrow \mu^+\mu^-/\tau^+\tau^-)}{\Gamma(h \rightarrow \mu^+\mu^-/\tau^+\tau^-)_{SM}} \quad (26)$$

$$\mu_{\gamma\gamma} = \frac{\Gamma(h \rightarrow \gamma\gamma)}{\Gamma(h \rightarrow \gamma\gamma)_{SM}}, \quad (27)$$

for the decay factors, where $VV^* = WW^*$, ZZ^* and the RPC hVV and hbb couplings, g_{hVV}^{RPC} and g_{hbb}^{RPC} , as well as the decay widths for $h \rightarrow gg$, $\gamma\gamma$, $\mu^+\mu^-$, $\tau^+\tau^-$ are given in Appendix A. In particular, the hV and VBF production channels as well as the Higgs decays to a pair of W and Z bosons are not changed in our BRPV setup (i.e., in the no-VEV basis $\langle \tilde{\nu}_\tau \rangle = 0$) with respect to the RPC SUSY framework. For the total Higgs width in the RPV SUSY scenario we add the new decay channels $h \rightarrow \tau^\pm \chi_2^\mp$ and $h \rightarrow \nu_\tau \tilde{\chi}_2^0$ when they are kinematically open (see next section).

³ We neglect Higgs production via $pp \rightarrow t\bar{t}h$, which, although included in the ATLAS and CMS fits, is 2-3 orders of magnitudes smaller than the gluon-fusion channel. Note that additional sources of Higgs production via heavy SUSY scalar decays may be present as well [91].

Finally, in the numerical simulations presented below we use the combined ATLAS and CMS signal strength measurements (at 13 TeV) which are listed in Table I.

IV. BILINEAR RPV - NUMERICAL RESULTS

To quantify the impact of BRPV on the 125 GeV Higgs physics we performed a numerical simulation, evaluating all relevant Higgs production and decays modes under the following numerical and parametric setup (for recent work in this spirit see [47, 48]):

- Our relevant input parameters are $(\mu, M_1, M_2, t_\beta, m_A, m_{\tilde{\nu}_\tau}, m_{\tilde{q}}, \tilde{A}, m_{\tilde{b}_{RR}}, m_{\tilde{\tau}_{RR}}, \delta_\epsilon, \delta_B)$, where $m_{\tilde{q}}$ is used as a common left-handed (soft) squark mass (i.e., $m_{\tilde{q}}\tilde{q}_L^*\tilde{q}_L$) for both the stop and sbottom states (see Appendix A 3) and $t_\beta \equiv \tan \beta$.
- In the stop sector we have assumed a degeneracy between the right and left-handed soft masses, i.e., $m_{\tilde{t}_{RR}} = m_{\tilde{q}}$; this is also used in the calculation of the stop-top loop corrections to the CP-even scalar mass matrix, see [88]. On the other hand, in the sbottom and stau sectors we keep the right-handed soft mass terms, $m_{\tilde{b}_{RR}}, m_{\tilde{\tau}_{RR}}$, as free-parameters.
- We adopt the Minimal Flavor Violation (MFV) setup for the squarks and sleptons soft trilinear terms, assuming that they are proportional to the corresponding Yukawa couplings: $A_f = y_f \cdot \tilde{A}$, for $f = t, b, \tau$.⁴ We thus vary the common trilinear soft term \tilde{A} for all the squarks and sleptons states.
- We randomly vary the model input parameters $(\mu, M_1, M_2, t_\beta, m_A, m_{\tilde{\nu}_\tau}, m_{\tilde{q}}, \tilde{A}, m_{\tilde{b}_{RR}}, m_{\tilde{\tau}_{RR}}, \delta_\epsilon, \delta_B)$ within fixed ranges which are listed in Table II. In some instances and depending on the RPV scenario analyzed below, these ranges are refined for the purpose of optimizing the BRPV effect, thereby focusing on more specified regions of the RPV SUSY parameter space.
- In cases where the Higgs decays to gauginos, we consider light gaugino states with a mass $\sim 90 - 100$ GeV (see e.g. [93]), which requires a higgsino mass parameter μ and/or gaugino mass parameters $M_{1,2}$ of $\mathcal{O}(100 \text{ GeV})$.
- We impose the following set of "filters" and constraints to ensure viable model configurations:

Higgs mass: We fix the lightest Higgs mass to its observed value $m_h^{obs} \simeq 125$ GeV in the computation of the Higgs production and decay rates. Nonetheless, we allow for a theoretical uncertainty of ± 3 GeV in the calculated Higgs mass (leaving some room for other possible SUSY contributions that are not accounted for in our minimal RPV SUSY framework), thus requiring that $122 \text{ GeV} < m_h^{calc} < 128 \text{ GeV}$. In particular, we include in m_h^{calc} the leading top-stop corrections (see Eq. (11)) and the sbottom and stau 1-loop contributions (which are not explicitly added in Eq. (11) but can be relevant for large $\tan \beta$ [94]):

$$(\Delta m_h^2)_{\tilde{f}} \approx -\frac{N_c^{\tilde{f}}}{\sqrt{2}G_F} \frac{y_f}{96\pi^2} \frac{\mu^4}{m_{\tilde{f}}^2}, \quad (28)$$

where here $\tilde{f} = \tilde{b}, \tilde{\tau}$, $N_c^{\tilde{b}} = 3$, $N_c^{\tilde{\tau}} = 1$, $m_{\tilde{b}}^2 = m_{\tilde{b}_1} \cdot m_{\tilde{b}_2}$ and $m_{\tilde{\tau}}^2 = m_{\tilde{\tau}_2} \cdot m_{\tilde{\tau}_3}$ and it is understood that $m_{\tilde{\tau}_2}$ and $m_{\tilde{\tau}_3}$ are the masses of the two lightest slepton states ($\tilde{\tau}_1$ being the massless Goldstone boson).

Neutrino masses: The RPV parameters are subject to constraints from various processes [95], such as flavor violating b -decays $b \rightarrow s\gamma$ [96–99] and Higgs decays [45], as well as radiative leptonic decays, e.g., $\mu \rightarrow e\gamma$ [100, 101]. Other notable quantities that are sensitive to the RPV parameter-space constraints are, e.g., Electric Dipole Moments (EDM's) [102–107] and neutrino masses [26–28, 30–32, 34]. A recent paper reviewing the various constraints on the RPV parameter-space is given in [46] and bounds on the TRPV couplings can be found in [60, 108].

We find that the strongest constraints on the BRPV parameters δ_B and δ_ϵ are from neutrino masses. In particular, neutrino masses can be generated at tree-level when only $\delta_\epsilon \neq 0$ and at the 1-loop level if also $\delta_B \neq 0$. In the former case $m_\nu \propto \delta_\epsilon^2$, while at 1-loop $m_\nu \propto \delta_B \delta_\epsilon, \delta_B^2$, see [34]. For example, the δ_B^2 1-loop

⁴ For the fermion Yukawa couplings we have $y_f = \frac{\sqrt{2}m_f}{vc_\beta}$ for the down-type quarks and leptons and $y_f = \frac{\sqrt{2}m_f}{vs_\beta}$ for up-type quarks.

contribution to the neutrino masses, which enters in eq. (15) is [34] (for the expression of $(m_{\nu_\tau})_{loop}^{\delta_B \delta_\epsilon}$ which is rather lengthy we refer the reader to [34]):

$$\begin{aligned}
(m_{\nu_\tau})_{loop}^{\delta_B \delta_\epsilon} = & \sum_{\alpha=1}^4 \frac{\left(\frac{\delta_B m_A^2 s_{2\beta}}{2}\right)^2}{4c_\beta^2} (g_2 U_{\alpha 2}^{RPC} - g_1 U_{\alpha 1}^{RPC})^2 m_{\tilde{\chi}_\alpha} \\
& \times \left[I_4(m_h, m_{\tilde{\nu}_\tau}, m_{\tilde{\nu}_\tau}, m_{\tilde{\chi}_\alpha}) \left(1 - (c_\beta Z_{h1} + s_\beta Z_{h2})^2\right) \right. \\
& \left. + I_4(m_H, m_{\tilde{\nu}_\tau}, m_{\tilde{\nu}_\tau}, m_{\tilde{\chi}_\alpha}) (c_\beta Z_{h1} + s_\beta Z_{h2})^2 - I_4(m_A, m_{\tilde{\nu}_\tau}, m_{\tilde{\nu}_\tau}, m_{\tilde{\chi}_\alpha}) \right] \quad (29)
\end{aligned}$$

where U^{RPC} is the neutralino mixing matrix in the RPC limit (i.e., corresponding to m_N^{RPC} which is the 4×4 RPC block in (15)), $m_{\tilde{\chi}_\alpha}$ are the neutralino masses in the RPC case, i.e., $\alpha = 1, 2, 3, 4$, and I_4 is defined in [34]. Also, we have used our definition for the BRPV parameter δ_B in eq. (8) and $s_{\alpha-\beta}^2 = (c_\beta Z_{h1} + s_\beta Z_{h2})^2$. Furthermore, m_H is the mass of the heavy CP-even Higgs state and $m_{\tilde{\nu}_\tau}$ is the sneutrino mass.

We use below the current Laboratory bounds on the muon and τ -neutrino masses: $m_{\nu_\mu} < 0.19$ MeV and $m_{\nu_\tau} < 18.2$ MeV [109]. In particular, in our numerical simulations, we evaluate the contribution of δ_B and δ_ϵ to the relevant neutrino mass for each run, i.e., calculating $(m_{\nu_\tau})_{loop}^{\delta_B \delta_\epsilon}$ and $(m_{\nu_\tau})_{loop}^{\delta_B \delta_\epsilon}$ and requiring the lightest physical neutralino state ($\tilde{\chi}_1^0 = \nu_\mu$ or $\tilde{\chi}_1^0 = \nu_\tau$ depending on the RPV scenario considered, see eq. (15)) to have a mass below these bounds.

We note that neutrino oscillation data and cosmology, imply tighter indirect bounds on neutrino masses; at the sub-eV range [110]. These bounds are, however, model dependent and they apply when interpreted within the SM of particle physics and the standard cosmological framework. In particular, oscillation data constrain the differences between the square of the neutrino masses, $\Delta m_{ij}^2 = m_{\nu_i}^2 - m_{\nu_j}^2$, and therefore it does not exclude scenarios with e.g., degenerate MeV-scale neutrinos. If indeed the neutrino mass scale is at the MeV range, for example, then a fine-tuning of the order of $\mathcal{O}(10^{-12})$ in the neutrino mass squared differences is required in order to accommodate the neutrino oscillation data measurements or, alternatively, some underlying flavor symmetry within a model may be responsible for $\Delta m_{ij}^2 \ll m_{i,j}^2$. It should be noted, though, that even without a flavor model, a fine tuning of $\mathcal{O}(10^{-12})$ should not be dismissed a priori since comparable and even more severe fine-tuning is currently observed in nature, e.g., in the fermion mass spectrum, in the gauge-Higgs sector and in the cosmological constant. In that respect we note that the purpose of this paper is not to reconstruct the neutrino oscillation data within a given flavor model but rather to study the impact of RPV SUSY on the Higgs signals under an unbiased and model independent manner using direct constraints on the RPV parameters.

The cosmological bounds (from Big Bang Nucleosynthesis, the power spectrum of the Cosmic Microwave Background anisotropies and the large scale clustering of cosmological structures), assume the minimal Λ CDM cosmological model and the standard neutrino decoupling process, i.e., involving only weak interactions, so that the only massless or light (sub-keV) relic particles since the Big Bang Nucleosynthesis (BBN) epoch are assumed to be photons and stable active neutrinos. Thus, the cosmology bounds do not apply within extended scenarios involving extra light particles (relics) or unstable neutrinos with a relative short life-time [111–115] and/or new neutrino interactions [116, 117] which open up new neutrino annihilation channels in the early universe. In fact, the RPV framework itself is one interesting example for a scenario that can potentially change the cosmological picture and thus evade the cosmology bounds on the neutrino masses. In particular, if R-Parity is spontaneously broken [118–120], then the theory contains a massless Goldstone boson (usually referred to as the Majoron and denoted by J) and the left-handed neutrinos can decay invisibly⁵ via $\nu_i \rightarrow \nu_j + J$ (i.e., $m_{\nu_i} > m_{\nu_j}$), thus evading the critical density argument against MeV-scale neutrino and, furthermore, possibly evading the BBN constraints due to the new annihilation channel $\nu\nu \rightarrow JJ$. Other interesting BSM scenarios that can avoid or significantly alleviate the cosmological bounds on the neutrino masses can be found e.g., in the $\tilde{\nu}$ -neutrinoless universe⁶ of [129] and in [130–132] in which new physics in the neutrino sector was assumed.

Let us furthermore comment on the neutrinoless double-beta ($0\nu\beta\beta$) bounds on the effective electron-neutrino mass. In the RPV SUSY framework, the $0\nu\beta\beta$ decay amplitude receives additional contributions from SUSY particles (sleptons, charginos, neutralinos, squarks and gluinos), which do not involve the

⁵ Note that current bounds on invisible decays of neutrinos from solar neutrino and neutrino oscillation experiments are rather weak [121–128].

TABLE II: Initial input parameter ranges for the free-parameters in the numerical simulations. See also text.

	Range
δ_ϵ	[0, 0.5]
μ	[90, 1000] [GeV]
M_1	[100, 2500] [GeV]
M_2	[100, 2500] [GeV]
t_β	[2, 30]
δ_B	[0, 0.5]
m_A	[1000, 10000] [GeV]
$m_{\tilde{\nu}_\tau}$	[200, 800] [GeV]
$m_{\tilde{q}}$	[1000, 8000] [GeV]
\tilde{A}	[0, 4000] [GeV]
$m_{\tilde{b}_{RR}}$	[2000, 5000] [GeV]
$m_{\tilde{\tau}_{RR}}$	[1000, 5000] [GeV]

Majorana neutrino exchange mechanism, see e.g., [133, 134]. Thus, any physics output of the $0\nu\beta\beta$ decay depends on the underlying assumption and/or SUSY parameter space. In particular, for a destructive interference between the neutrino exchange mechanism and the pure SUSY mechanisms, it seems plausible to find regions in parameter space, where no constraints from $0\nu\beta\beta$ decay could be derived on the effective electron-neutrino mass [134].

Higgs signals: For each point/model in our RPV SUSY parameter-space we calculate all the Higgs signal strengths in Table I and require them to agree with the measured ones at the 2σ level.

A. Higgs decays to Gauginos

We study here the pure BRPV Higgs decays $h \rightarrow \nu_\tau \tilde{\chi}_2^0$ and $h \rightarrow \tau^\pm \tilde{\chi}_2^\mp$, see also [42, 43] (for another interesting variation of RPV Higgs decays to gauginos see [52]). Depending on the scenario under consideration, we require $m_{\tilde{\chi}_2^0} < 125$ GeV and/or $m_{\tilde{\chi}_2^\mp} \lesssim 125$ GeV, in which case the BRPV decays $h \rightarrow \nu_\tau \tilde{\chi}_2^0$ and/or $h \rightarrow \tau^\pm \tilde{\chi}_2^\mp$ are kinematically open, respectively (also adding them to the total Higgs width Γ^h).

We consider four BRPV scenarios for the parameter space associated with the gaugino sector:

- S1A:** A gaugino-like scenario with $M_2 \ll \mu$ [135], and nearly degenerate 2nd lightest neutralino and chargino with a mass lighter than the Higgs mass: $m_{\tilde{\chi}_2^0} \simeq m_{\tilde{\chi}_2^\mp} < 125$ GeV. In this case, both decays $h \rightarrow \nu_\tau \tilde{\chi}_2^0$ and $h \rightarrow \tau^\pm \tilde{\chi}_2^\mp$ are kinematically allowed.
- S1B:** A higgsino-like scenario with $\mu \ll M_2$ [135], and nearly degenerate 2nd lightest neutralino and chargino with a mass lighter than the Higgs mass: $m_{\tilde{\chi}_2^0} \simeq m_{\tilde{\chi}_2^\mp} < 125$ GeV. In this case also, both decays $h \rightarrow \nu_\tau \tilde{\chi}_2^0$ and $h \rightarrow \tau^\pm \tilde{\chi}_2^\mp$ are kinematically open.
- S2:** No degeneracy in the gaugino sector with $m_{\tilde{\chi}_2^0} < 125$ GeV and $m_{\tilde{\chi}_2^\mp} > 125$ GeV, so that only the decay channel $h \rightarrow \nu_\tau \tilde{\chi}_2^0$ is kinematically open.
- S3:** No degeneracy in the gaugino sector with both $m_{\tilde{\chi}_2^0}, m_{\tilde{\chi}_2^\mp} < 125$ GeV and a significant branching fraction in the neutralino channel $h \rightarrow \nu_\tau \tilde{\chi}_2^0$: $BR(h \rightarrow \nu_\tau \tilde{\chi}_2^0) \gtrsim 10\%$ and a kinematically open $h \rightarrow \tau^\pm \tilde{\chi}_2^\mp$ decay with much smaller rate.

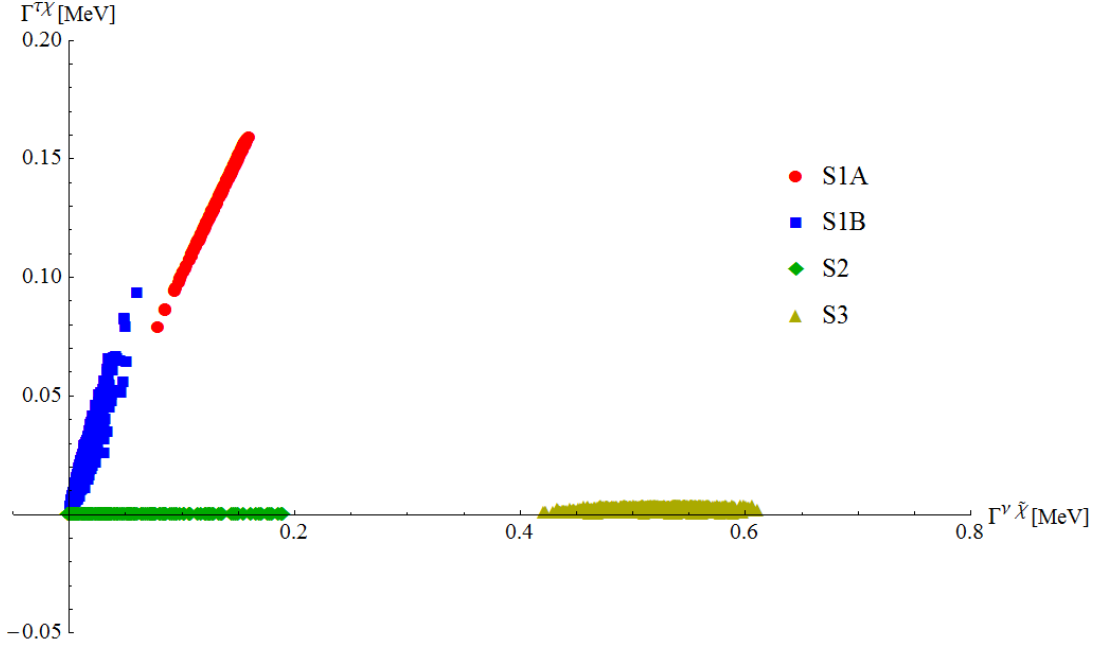


FIG. 1: A scatter plot in the $(\Gamma^{\nu\tilde{\chi}}, \Gamma^{\tau\tilde{\chi}})$ plane for the four proposed BRPV scenarios: **S1A**, **S1B**, **S2** and **S3**, see text.

We give in Fig. 1 a scatter plot of the surviving model configurations in the $\Gamma^{\nu\tilde{\chi}}-\Gamma^{\tau\tilde{\chi}}$ plane for the above four BRPV scenarios, where $\Gamma^{\nu\tilde{\chi}} = \Gamma(h \rightarrow \nu_\tau \tilde{\chi}_2^0)$ and $\Gamma^{\tau\tilde{\chi}} = \Gamma(h \rightarrow \tau^\pm \tilde{\chi}_2^\mp)$. We can see that within the two **S1** scenarios, **S1A** yields larger decay rates in both channels $h \rightarrow \nu_\tau \tilde{\chi}_2^0$ and $h \rightarrow \tau^\pm \tilde{\chi}_2^\mp$, in particular, reaching a width $\Gamma^{\nu\tilde{\chi}} \sim \Gamma^{\tau\tilde{\chi}} \sim 0.1 - 0.2$ MeV. In the **S2** scenario we expect a BRPV signal only in the $h \rightarrow \nu_\tau \tilde{\chi}_2^0$ channel ($h \rightarrow \tau^\pm \tilde{\chi}_2^\mp$ is kinematically closed, see above), which can also reach a width of $\Gamma^{\nu\tilde{\chi}} \sim 0.2$ MeV. Finally, we see that the **S3** scenario is expected to give the largest BRPV decay rate in the neutralino channel $h \rightarrow \nu_\tau \tilde{\chi}_2^0$, reaching $\Gamma(h \rightarrow \nu_\tau \tilde{\chi}_2^0) \sim \mathcal{O}(0.5)$ MeV, which is more than 10% of the total SM Higgs width; in this case, the BRPV Higgs decay channel to a chargino, $h \rightarrow \tau^\pm \tilde{\chi}_2^\mp$ is effectively closed due to a limited phase-space. We thus see that the different **Si** SUSY scenarios that we have outlined above, probe different regions in the $\Gamma^{\nu\tilde{\chi}}-\Gamma^{\tau\tilde{\chi}}$ BRPV Higgs decays plane, where the cases without the $\tilde{\chi}_2^0 - \tilde{\chi}_2^\pm$ mass degeneracy (scenarios **S2** and **S3**) we obtain a better sensitivity to the neutralino channel $h \rightarrow \nu_\tau \tilde{\chi}_2^0$.

In Table III we list four representative benchmark models **BMi** (i.e., sets of input parameters) which correspond to the four **Si** scenarios considered above. These sample benchmark models maximize the BRPV effect (i.e., decay rates) associated with the **Si** scenarios; the corresponding BRPV Higgs decay width into a single neutralino and a single chargino are given in Table IV. As can be seen from Table III, all four **BM** models require low $t_\beta \sim 2 - 3$. Note also that **BM3**, for which we obtain a width of $\Gamma(h \rightarrow \nu_\tau \tilde{\chi}_2^0) \sim \mathcal{O}(0.6)$ MeV (see Table IV) is characterized by the hierarchy $\mu \sim M_1 \ll M_2$ in the gaugino sector.

Another useful handle that can help distinguish between the BRPV benchmark models is the set of 125 GeV Higgs signals considered in section III. In Table V we list the predicted Higgs signal strengths for the selected benchmark models. Indeed, we see that large deviations of $\mathcal{O}(25\%)$ are expected in the **BM1A** scenario in the di-photon channels $\mu_{F\gamma\gamma}^{(gg)}$ and $\mu_{V\gamma\gamma}^{(VBF)}$, due to the contribution of the light charginos in this case (see Table XIII). In contrast, in the **BM1B** scenario, a large effect of $\mathcal{O}(20\%)$ is expected in $h \rightarrow \tau\tau$ channels $\mu_{F\tau\tau}^{(gg)}$ and $\mu_{V\tau\tau}^{(VBF)}$. Furthermore, while the **BM2** setup does not exhibit significant deviations from the SM, the Higgs signal strengths in the $h \rightarrow \tau^+\tau^-$ and $h \rightarrow b\bar{b}$ channels, $\mu_{F\tau\tau}^{(gg)}$, $\mu_{V\tau\tau}^{(VBF)}$ and $\mu_{Vb\bar{b}}^{(hV)}$, exhibit non-negligible sensitivity to the benchmark model **BM3**. It is also worth noting that in all four benchmark models $\mu_{FWW}^{(gg)} = \mu_{FZZ}^{(gg)} = 0.92$ (recall that in our BRPV framework we have $\mu_{FWW}^{(gg)} = \mu_{FZZ}^{(gg)}$), thus saturating the 2σ lower bound in these channels (see Table I).

Finally, we wish to briefly comment on the experimental signatures of the BRPV decays $h \rightarrow \nu_\tau \tilde{\chi}_2^0$ and/or $h \rightarrow \tau^\pm \tilde{\chi}_2^\mp$ considered in this section. For this purpose, we compute the subsequent chargino and neutralino decays in our BRPV SUSY framework. In particular, the leading decays of the 2nd lightest gauginos in the BRPV scenario are the 2-body $\tilde{\chi}_2^+ \rightarrow \nu W^+$, $\tilde{\chi}_2^+ \rightarrow \tau^+ Z$ and $\tilde{\chi}_2^0 \rightarrow \tau^- W^+$, $\tilde{\chi}_2^0 \rightarrow \nu Z$ [136–139], since the 3-body sfermion-mediated gaugino decays (see e.g., [45, 140]) are suppressed by both an extra RPV small coupling and a heavy off-shell sfermion propagator (in the heavy SUSY limit used in this work). In particular, we find that for all the above benchmark models, the gauginos

TABLE III: Input parameters for the selected benchmark models: BM1A, BM1B, BM2 and BM3, see text.

	BM1A	BM1B	BM2	BM3	
δ_ϵ	0.04	0.27	0.10	0.22	
μ	626.54	92.90	220.38	120.05	[GeV]
M_1	523.19	2030.48	104.94	130.56	[GeV]
M_2	103.83	1028.05	991.55	999.39	[GeV]
t_β	2.14	2.73	2.81	3.15	
δ_B	0.05	0.11	0.17	0.10	
m_A	4467.78	2558.96	2710.2	3162.6	[GeV]
$m_{\tilde{\nu}_\tau}$	291.65	317.38	506.78	358.69	[GeV]
$m_{\tilde{q}}$	6071.69	2860.5	4628.27	1094.07	[GeV]
\tilde{A}	1537.44	2842.51	66.19	3180.91	[GeV]
$m_{\tilde{b}_{RR}}$	4814.49	4996.39	4245.07	4721.63	[GeV]
$m_{\tilde{\tau}_{RR}}$	1509.25	1303.96	1122.68	2670.45	[GeV]

TABLE IV: The BRPV decay width for the selected benchmark models: BM1A, BM1B, BM2 and BM3, see text.

	BM1A	BM1B	BM2	BM3	
$\Gamma^{\nu\tilde{\chi}}$	0.159	0.06	0.189	0.61	[MeV]
$\Gamma^{\tau\tilde{\chi}}$	0.158	0.09	0	0.002	[MeV]

decay almost exclusively to final states involving the W -boson, with branching ratios $BR(\chi_2^+ \rightarrow \nu W^+)$, $BR(\tilde{\chi}_2^0 \rightarrow \tau^- W^+) \gtrsim 90\%$. Furthermore, these gaugino 2-body BRPV decays are prompt with a lifetime corresponding to $l \sim 10^{-10}$ m, i.e., they decay within the detector. As a result, the expected signals for both $h \rightarrow \nu_\tau \tilde{\chi}_2^0$ and $h \rightarrow \tau^\pm \chi_2^\mp$ (after the subsequent decays of the W) include e.g., a pair of opposite charged non-diagonal leptons $\tau^\pm e^\mp$ and/or $\tau^\pm \mu^\mp$ as well as a pair of opposite charged τ -leptons with accompanying missing energy: $h \rightarrow \tau^\pm \chi_2^\mp \rightarrow \tau^\pm \ell^\mp + \cancel{E}_T$

TABLE V: The Higgs observables for the selected benchmark models: BM1A, BM1B, BM2 and BM3 (see text).

	BM1A	BM1B	BM2	BM3
$\mu_{F\gamma\gamma}^{(gg)}$	1.24	1.09	0.99	1.01
$\mu_{FZZ}^{(gg)}$	0.92	0.92	0.92	0.92
$\mu_{FWW}^{(gg)}$	0.92	0.92	0.92	0.92
$\mu_{F\tau\tau}^{(gg)}$	0.91	0.77	0.92	0.82
$\mu_{F\mu\mu}^{(gg)}$	0.92	0.97	0.96	0.96
$\mu_{Vbb}^{(hV)}$	0.92	0.98	0.97	0.88
$\mu_{V\gamma\gamma}^{(VBF)}$	1.24	1.10	1.00	0.93
$\mu_{V\tau\tau}^{(VBF)}$	0.92	0.78	0.93	0.75

and $h \rightarrow \nu_\tau \tilde{\chi}_2^0 \rightarrow \tau^\pm \ell^\mp + \cancel{E}_T$, where $\ell = e, \mu, \tau$. Let us therefore define the following decay signal:

$$\mu_{\tau\ell+\cancel{E}_T} \equiv \frac{\Gamma(h \rightarrow \tau^\pm \ell^\mp + \cancel{E}_T)}{\Gamma(h \rightarrow \tau^\pm \ell^\mp + \cancel{E}_T)_{SM}}, \quad (30)$$

where the dominant underlying Higgs decay in the SM is:⁶

$$\Gamma(h \rightarrow \tau^\pm \ell^\mp + \cancel{E}_T)_{SM} = \Gamma(h \rightarrow WW^* \rightarrow \tau^\pm \ell^\mp + \cancel{E}_T)_{SM}; \quad \ell = e, \mu, \tau, \quad (31)$$

while in our BRPV SUSY framework we have:

$$\begin{aligned} \Gamma(h \rightarrow \tau^\pm \ell^\mp + \cancel{E}_T) &= \Gamma(h \rightarrow WW^* \rightarrow \tau^\pm \ell^\mp + \cancel{E}_T) + \Gamma(h \rightarrow \tau^\pm \chi_2^\mp \rightarrow \tau^\pm \ell^\mp + \cancel{E}_T) \\ &+ \Gamma(h \rightarrow \nu_\tau \tilde{\chi}_2^0 \rightarrow \tau^\pm \ell^\mp + \cancel{E}_T); \quad \ell = e, \mu, \tau. \end{aligned} \quad (32)$$

In particular, we have $\Gamma(h \rightarrow WW^* \rightarrow \tau^\pm \ell^\mp + \cancel{E}_T) = (g_{hVV}^{RPC})^2 \Gamma(h \rightarrow WW^* \rightarrow \tau^\pm \ell^\mp + \cancel{E}_T)_{SM}$ (see eq. (A1)) so that

$$\mu_{\tau\ell+\cancel{E}_T} = (g_{hVV}^{RPC})^2 + \frac{\Gamma(h \rightarrow \tau^\pm \chi_2^\mp \rightarrow \tau^\pm \ell^\mp + \cancel{E}_T) + \Gamma(h \rightarrow \nu_\tau \tilde{\chi}_2^0 \rightarrow \tau^\pm \ell^\mp + \cancel{E}_T)}{\Gamma(h \rightarrow WW^* \rightarrow \tau^\pm \ell^\mp + \cancel{E}_T)_{SM}}, \quad (33)$$

where the second term in eq. (33) above is a pure BRPV effect.

We can thus evaluate this BRPV decay signal, $\mu_{\tau\ell+\cancel{E}_T}$, in our four benchmark models BM1A, BM1B, BM2 and BM3. In particular, in all these benchmark models we have $\mu_{FWW}^{(gg)} \sim (g_{hVV}^{RPC})^2 \sim 0.92$, whereas $\Gamma(h \rightarrow \tau^\pm \chi_2^\mp) + \Gamma(h \rightarrow \nu_\tau \tilde{\chi}_2^0) \sim 0.3, 0.15, 0.2, 0.6$ in the benchmark models BM1A, BM1B, BM2 and BM3, respectively (see Table IV). Furthermore, as mentioned above, in all four BMi we have $BR(\chi_2^+ \rightarrow \nu W^+) \gtrsim 0.9$ and $BR(\tilde{\chi}_2^0 \rightarrow \tau^- W^+) \gtrsim 0.9$. We thus expect $\Gamma(h \rightarrow \tau^\pm \chi_2^\mp \rightarrow \tau^\pm \ell^\mp + \cancel{E}_T) + \Gamma(h \rightarrow \nu_\tau \tilde{\chi}_2^0 \rightarrow \tau^\pm \ell^\mp + \cancel{E}_T) \sim 0.015 - 0.06$ MeV depending on the benchmark model, while in the SM we have $\Gamma(h \rightarrow WW^* \rightarrow \tau^\pm \ell^\mp + \cancel{E}_T)_{SM} \sim 0.01$ MeV (recall that $BR(W \rightarrow \ell \nu_\ell) \sim 1/9$ in any single lepton decay channel of the W), so that, overall, we expect that the BRPV SUSY models described above will yield:

$$\mu_{\tau\ell+\cancel{E}_T} \equiv \frac{\Gamma(h \rightarrow \tau^\pm \ell^\mp + \cancel{E}_T)}{\Gamma(h \rightarrow \tau^\pm \ell^\mp + \cancel{E}_T)_{SM}} \sim 2.5 - 7, \quad (34)$$

which is **several times larger than** the signal expected in the SM or in the RPC SUSY case: $\mu_{\tau\ell+\cancel{E}_T} \sim (g_{hVV}^{RPC})^2 \sim 0.92$.

B. Higgs decay to a pair of leptons: $h \rightarrow \mu^+ \mu^-$ and $h \rightarrow \tau^+ \tau^-$

In the RPC SUSY framework the Higgs decays to a pair of τ -leptons and muons are governed by the corresponding Yukawa couplings and are sensitive to the parameters in the Higgs sector, i.e., to $\tan\beta$ and the pseudoscalar Higgs mass m_A [17] (at tree-level). In particular, in the so called decoupling limit where $m_A^2 \gg m_Z^2$, the Higgs decays into these channels have rates very similar to the SM rates, so that the corresponding signal strengths are expected to be $\mu_{F\tau\tau}^{(gg)}, \mu_{F\mu\mu}^{(gg)} \rightarrow 1$. Note that the Higgs decay to a pair of τ -leptons is also sensitive to the Higgs signal $\mu_{V\tau\tau}^{(VBF)}$, which is also expected to be $\mu_{V\tau\tau}^{(VBF)} \rightarrow 1$ since $\mu_V^{(VBF)} \sim 1$ (see eq. 23) at decoupling [17].

On the other hand, when the BRPV interactions are "turned on", additional diagrams can contribute to these decays, yielding $\delta_\epsilon \cdot \delta_B$ (see e.g., diagram (b) in Fig. 4) and/or $(\delta_\epsilon)^2$ BRPV effects. We have performed another numerical search for models that maximize the BRPV effects in the decays $h \rightarrow \mu^+ \mu^-$ and $h \rightarrow \tau^+ \tau^-$, within the ranges of input parameters used in Table II and the filters described above. In particular, for the case of $h \rightarrow \mu^+ \mu^-$ we assume that the BRPV interactions involves the 2nd generation lepton and slepton, so that in this case we assume that δ_ϵ parameterizes $\mu - \chi^+$ mixing and δ_B is responsible for $\tilde{\nu}_\mu - h$ mixing. Also, we have modified the neutrino mass bound filter in the $h \rightarrow \mu^+ \mu^-$ case accordingly to $m_{\nu_\mu} < 0.19$ MeV [109]. We note that a better sensitivity to the BRPV effect in the leptonic Higgs decays, $h \rightarrow \tau^+ \tau^-$, $\mu^+ \mu^-$, is obtained when the Higgs decay channels to gauginos $h \rightarrow \nu_\tau \tilde{\chi}_2^0$ and $h \rightarrow \tau^\pm \chi_2^\mp$ are kinematically closed, i.e., when $m_{\tilde{\chi}_2^0}, m_{\chi_2^\pm} > m_h$.

In Table VI we list two representative benchmark models, BM τ and BM μ , for which we find a substantial deviation from $\mu_{F\tau\tau}^{(gg)} = \mu_{V\tau\tau}^{(VBF)} = 1$ and $\mu_{F\mu\mu}^{(gg)} = 1$, respectively (as mentioned earlier, the RPC SUSY effect on the 125 GeV

⁶ The contribution of the decay $h \rightarrow ZZ^*$ to the $\tau^\pm \ell^\mp + \cancel{E}_T$ signal is subdominant and has a different kinematical signature.

TABLE VI: Input parameter sets for the benchmark models $\text{BM}\mu$ and $\text{BM}\tau$, with $l = \mu$ and $l = \tau$, respectively, for the parameters $m_{\tilde{\nu}_l}$ and $m_{\tilde{l}_{RR}}$, see also text.

	$\text{BM}\mu$	$\text{BM}\tau$	
δ_ϵ	0.47	0.49	
μ	642.71	631.61	[GeV]
M_1	1426.05	1651.6	[GeV]
M_2	682.82	687.75	[GeV]
t_β	6.31	6.76	
δ_B	0.05	0.05	
m_A	8981.82	8530.08	[GeV]
$m_{\tilde{\nu}_l}$	543.82	535.47	[GeV]
$m_{\tilde{q}}$	2210.72	2415.51	[GeV]
\tilde{A}	520.38	247.83	[GeV]
$m_{\tilde{b}_{RR}}$	4720.75	4594.09	[GeV]
$m_{\tilde{l}_{RR}}$	4249.44	4145.23	[GeV]

TABLE VII: The Higgs signal strength observables corresponding to the benchmark models $\text{BM}\mu$ and $\text{BM}\tau$, see text.

	$\text{BM}\mu$	$\text{BM}\tau$
$\mu_{F\gamma\gamma}^{(gg)}$	1.00	1.02
$\mu_{FZZ}^{(gg)}$	0.98	1.00
$\mu_{FWW}^{(gg)}$	0.98	1.00
$\mu_{F\tau\tau}^{(gg)}$	0.99	0.73
$\mu_{F\mu\mu}^{(gg)}$	0.75	1.01
$\mu_{Vbb}^{(hV)}$	1.00	1.02
$\mu_{V\gamma\gamma}^{(VBF)}$	1.01	1.02
$\mu_{V\tau\tau}^{(VBF)}$	1.00	0.73

Higgs signals and in particular on the Higgs decays to a pair of leptons is negligible in the decoupling limit considered here). The resulting Higgs signal strength values corresponding to these two models are given in Table VII.

We see that the BRPV effects in $\text{BM}\tau$ and $\text{BM}\mu$ reduce the signal strengths in the lepton channels by about 25%, yielding $\mu_{F\tau\tau}^{(gg)} \sim \mu_{V\tau\tau}^{(VBF)} \sim 0.73$ and $\mu_{F\mu\mu}^{(gg)} \sim 0.75$, respectively, where these deviations from unity are primarily due to the BRPV lepton-chargino mixing parameter δ_ϵ , since $\delta_\epsilon \gg \delta_B$ in these benchmark models (see Table VI). This is still within the current 1σ error on the measured signal strength in $\mu_{F\tau\tau}^{(gg)}$ and $\mu_{F\mu\mu}^{(gg)}$ (see Table I), but may turn out to be an interesting signal of RPV SUSY when a precision of 5-10% will be reached on these quantities; in particular, since all other Higgs decay channels are left unchanged within the benchmark model $\text{BM}\mu$, whereas an interesting correlation $\mu_{F\tau\tau}^{(gg)} \sim \mu_{V\tau\tau}^{(VBF)}$ is obtained in $\text{BM}\tau$.

V. TRILINEAR RPV - NUMERICAL RESULTS

In this section we shortly explore some of the direct implications of TRPV interactions on the 125 GeV Higgs production and decay modes.⁷ In particular, we will consider below the four TRPV couplings λ'_{311} , λ'_{333} and λ_{322} , λ_{233} , which correspond to new TRPV $\tilde{\nu}_\tau \bar{d}d$ and $\tilde{\nu}_\tau \bar{b}b$ and $\tilde{\nu}_\tau \mu^+ \mu^-$ and $\tilde{\nu}_\mu \tau^+ \tau^-$ interactions, respectively, allowing also BRPV effects via $\delta_B \neq 0$ and assuming (throughout this section) that $\delta_\epsilon \ll \delta_B$, i.e., neglecting BRPV effects which are proportional to δ_ϵ .⁸ Indeed, the BRPV δ_B term mixes the Higgs with the sneutrino states, these new TRPV couplings can change the decay rates of the 125 GeV Higgs-sneutrino mixed state in the channels $h \rightarrow \bar{d}d, \bar{b}b, \mu^+ \mu^-, \tau^+ \tau^-$, so that the potential overall RPV effect is proportional to the product of the BRPV and TRPV couplings (at the amplitude level), i.e., to $\delta_B \cdot \lambda'$ or $\delta_B \cdot \lambda$, as we discuss next.

In the following numerical study, we again employ all the constraints/filters outlined in the previous section, i.e., Higgs mass, neutrino masses and Higgs signals. Here, however, the additional λ and λ' TRPV couplings give rise to new loop-induced contributions to the neutrino masses, so that the corresponding neutrino mass filters are modified accordingly. In particular, the leading contribution of the TRPV interactions to the neutrino mass arise at 1-loop and can be estimated via (see [34] for details):⁹

$$(m_{\nu_\tau})_{loop}^{\lambda'_{3ii} \lambda'_{3ii}} \sim \frac{3}{8\pi^2} (\lambda'_{3ii})^2 \frac{m_{q_i}^2}{\bar{m}_{\bar{q}_i}}, \quad (35)$$

where $m_{q_1} = m_d, m_{q_3} = m_b$ are the d and b -quark masses, respectively, and $\bar{m}_{\bar{q}_1}, \bar{m}_{\bar{q}_3} = \bar{m}_{\bar{d}}, \bar{m}_{\bar{b}}$ are the average masses of the sdown and the sbottom, respectively. Similarly, the 1-loop contributions for the λ_{233} and λ_{322} couplings are:

$$(m_{\nu_k})_{loop}^{\lambda_{kii} \lambda_{kii}} \sim \frac{1}{8\pi^2} (\lambda_{kii})^2 \frac{m_{\tilde{\ell}_i}^2}{\bar{m}_{\tilde{\ell}_i}}, \quad (36)$$

where here $m_{\nu_2} = m_{\nu_\mu}$ and $m_{\nu_3} = m_{\nu_\tau}$ and $\bar{m}_{\tilde{\ell}_2} = \bar{m}_{\tilde{\mu}}, \bar{m}_{\tilde{\ell}_3} = \bar{m}_{\tilde{\tau}}$ are the corresponding average masses of the muon and τ -neutrino charged slepton masses.

We note, however, that the above 1-loop pure TRPV corrections to the neutrino masses are sub-dominant in the scenarios considered below, i.e., with a multi-TeV squarks and charged sleptons spectrum; the largest effect arises from the λ'_{333} coupling, since it is proportional to the b -quark mass, see eq. (35).

A. The Higgs signals and $\delta_B \cdot \lambda'$ RPV effects

As schematically depicted in Fig. 2, when $\lambda'_{333} \neq 0$ the Higgs coupling to bottom quarks (see also eq. (A5)) receives a new TRPV term proportional to $\lambda'_{333} Z_{h3}$ (recall that $Z_{h3} = Z_{h3}(\delta_B)$):

$$\Lambda_{hbb} = g_b^{SM} \left(g_{hbb}^{RPC} + \frac{\lambda'_{333} Z_{h3}}{\sqrt{2} g_b^{SM}} \right) \quad (37)$$

where we have normalized the new TRPV contribution to the SM hbb coupling, $g_b^{SM} = \frac{m_b}{v}$, and denoted the RPC hbb coupling by $g_{hbb}^{RPC} \equiv \frac{Z_{h1}}{c_\beta}$ (see also eq. (A5)).

The new TRPV term in eq. (37) thus modifies (at tree-level) the Higgs decay $h \rightarrow b\bar{b}$:

$$\Gamma(h \rightarrow b\bar{b}) = 3 \frac{G_F m_b^2}{4\sqrt{2}\pi} \left(g_{hbb}^{RPC} + \frac{\lambda'_{333} Z_{h3}}{\sqrt{2} g_b^{SM}} \right)^2 m_h \left(1 - \frac{4m_b^2}{m_h^2} \right)^{\frac{3}{2}}, \quad (38)$$

and also the Higgs decays $h \rightarrow \gamma\gamma, gg$ at 1-loop. In particular, it modifies the 1-loop Higgs production in the gluon-fusion channel.¹⁰

Similar to the λ'_{333} effect in the hbb coupling, when $\lambda'_{311} \neq 0$ the couplings of the Higgs to a pair of d -quarks is also shifted by the term $(1/\sqrt{2})\lambda'_{311} Z_{h3}$. In this case however, the TRPV effect is manifest by an enhanced Higgs

⁷ We do not consider the corresponding soft-breaking TRPV terms, since these will contribute at higher orders and are therefore expected to yield smaller corrections to the Higgs observables.

⁸ We note that BRPV \times TRPV effects via $\delta_\epsilon \neq 0$ can have other interesting implications. For example, sbottom mixing can be altered by a $\delta_\epsilon \cdot \lambda'$ RPV term $\propto v\mu s_\beta \cdot (\delta_\epsilon \cdot \lambda'_{333})$, which in turn affects the contribution of sbottom exchange at 1-loop in the ggh and $\gamma\gamma h$ couplings, as well as the predicted Higgs mass (see eq. (28)).

⁹ There is an additional 1-loop BRPV \times TRPV contribution to the neutrino mass which is $\propto \delta_\epsilon \cdot \lambda'$ and which we do not consider here, assuming that it is much smaller by virtue of $\delta_\epsilon \rightarrow 0$.

¹⁰ The Higgs production via b -quark fusion, $b\bar{b} \rightarrow h$, is also modified by the extra TRPV term in eq.(37), but this channel is sub-dominant due to the small PDF content of the b, \bar{b} quarks in the proton and is, therefore, neglected here.

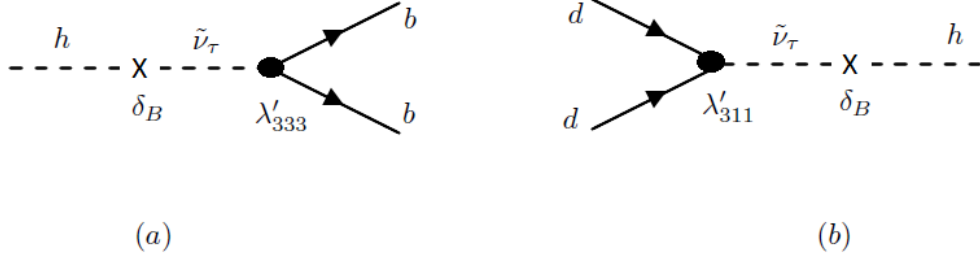


FIG. 2: Tree-level diagrams (couplings) that correspond to the main $\delta_B \cdot \lambda'$ effects in the Higgs decay $h \rightarrow b\bar{b}$ (diagram (a)) and in Higgs production via $d\bar{d}$ fusion (diagram (b)). The BRPV δ_B insertion is denoted by X whereas the new λ' TRPV interactions appear in bold vertices.

production mechanism via $d\bar{d}$ -fusion (see diagram (b) in Fig. 2); the corresponding TRPV effect in the Higgs decay $h \rightarrow d\bar{d}$ is not of our interest here since it is not yet measurable. Thus, in the presence of a non-zero TRPV λ'_{311} coupling we have (for the definition of the production factors $\mu_i^{(P)}$ see eqs. (21) and (22)):¹¹

$$\mu_F^{(gg+dd)} \equiv \frac{\sigma(gg \rightarrow h) + \sigma(d\bar{d} \rightarrow h)}{\sigma(gg \rightarrow h)_{SM}} = \mu_F^{(gg)} + \frac{\sigma(d\bar{d} \rightarrow h)}{\sigma(gg \rightarrow h)_{SM}}, \quad (39)$$

where the first term in eq. (39), $\mu_F^{(gg)}$, is the scaled gluon-fusion production factor in the RPV framework as defined in eq. (22) and calculated using eqs. (A22)–(A23).¹² The second term in eq. (39) requires special care, in particular, since the PDF's do not cancel out when taking the ratio. It is convenient to normalize the Higgs coupling to down quarks by the SM bottom-quark yukawa, $y_b = \sqrt{2}g_b^{SM} = \sqrt{2}m_b/v$ and adopt the coupling modifier formalism (“Kappa framework”), defining (see e.g., [141]):

$$\kappa_d^{TRPV} \equiv \frac{\lambda'_{311} Z_{h3}}{y_b}. \quad (40)$$

in which case the second term in eq. (39) can be written as:

$$\frac{\sigma(d\bar{d} \rightarrow h)}{\sigma(gg \rightarrow h)_{SM}} \simeq \frac{(\kappa_d^{TRPV})^2 \cdot \sigma(d\bar{d} \rightarrow h)_{\kappa_d^{TRPV}=1} \cdot K_d}{\sigma(gg \rightarrow h)_{SM}^{N3LO}} \simeq 0.73 (\kappa_d^{TRPV})^2, \quad (41)$$

where $\sigma(d\bar{d} \rightarrow h)_{\kappa_d^{TRPV}=1} \simeq 23.8$ [pb] [141], $\sigma(gg \rightarrow h)_{SM}^{N3LO} \simeq 48.6$ [pb] is the N3LO QCD prediction for the gluon-fusion Higgs production channel at the 13 TeV LHC [142] and $K_d \simeq 1.5$ is the estimated K-factor for the sub-process $d\bar{d} \rightarrow h$ with $\kappa_d^{TRPV} = 1$ [143].

In Tables VIII and IX we list the input parameters and the resulting Higgs signal strength observables for two benchmark models $\text{BM}\lambda'_{333}$ and $\text{BM}\lambda'_{311}$, setting $\lambda'_{333} \sim 0.5$ or $\lambda'_{311} \sim 1$, respectively, which correspond to the (conservative)¹³ upper bounds for squark masses above 1 TeV, see [95]. The benchmark model $\text{BM}\lambda'_{333}$ has been chosen to maximize the TRPV effect in the Higgs decay $h \rightarrow b\bar{b}$, while in $\text{BM}\lambda'_{311}$ the ratio in eq. (41) and, therefore, the Higgs production channel via $d\bar{d}$ -fusion are maximized.

Summarizing our results in Tables VIII and IX, we note that:

- The $\text{BM}\lambda'_{333}$ scenario exhibits only a mild enhancement in the $h \rightarrow b\bar{b}$ channel: $\mu_{Vbb}^{(hV)} = 1.04$. This implies that the Higgs decay channel $h \rightarrow b\bar{b}$ is dominated by the b -quark yukawa coupling, y_b , so that the new TRPV term in eq. (37) can be neglected in this case. On the other hand, the diphoton channels in the $\text{BM}\lambda'_{333}$ model are significantly enhanced: $\mu_{F\gamma\gamma}^{(gg)} \sim \mu_{V\gamma\gamma}^{(VBF)} \sim 1.25$, primarily due to the light chargino spectrum in this case (see Table XVI). Also, the vector boson decay channels saturate their 2σ lower bound in the $\text{BM}\lambda'_{333}$ scenario, i.e., $\mu_{FZZ}^{(gg)} \sim \mu_{FWW}^{(gg)} \sim 0.92$.

¹¹ We set $\sigma(d\bar{d} \rightarrow h)_{SM} = 0$ in eq. (39).

¹² The TRPV effect of the d -quark loop (via the λ'_{311} coupling) in the gluon-fusion channel is negligible, see e.g., [141].

¹³ The bounds on the TRPV parameters λ, λ' scale as $1/m_{\tilde{f}_R}$ [95] and can, therefore, be relaxed for $m_{\tilde{f}_R} > 1$ TeV (as assumed here). These bounds are also model-dependent, see e.g., [144].

TABLE VIII: Input parameters for the selected benchmark models $\text{BM}\lambda'_{333}$ and $\text{BM}\lambda'_{311}$. See also text.

	$\text{BM}\lambda'_{333}$	$\text{BM}\lambda'_{311}$	
δ_ϵ	0	0	
μ	202.46	556.34	[GeV]
M_1	759.74	1747.98	[GeV]
M_2	251.55	1589.49	[GeV]
t_β	2.77	16.59	
δ_B	0.11	0.45	
m_A	2150.46	1508.96	[GeV]
$m_{\tilde{\nu}_\tau}$	768	723.75	[GeV]
$m_{\tilde{q}}$	3461.04	2008.27	[GeV]
\tilde{A}	953.94	2.89	[GeV]
$m_{\tilde{b}_{RR}}$	2764.42	2421.53	[GeV]
$m_{\tilde{\tau}_{RR}}$	2357.42	3693.50	[GeV]

- In the $\text{BM}\lambda'_{311}$ scenario we have $\kappa_d^{TRPV} \sim 1.34$, so that the enhancement in the $d\bar{d} \rightarrow h$ production channel, see eq. (41), causes the (previously) gluon-fusion Higgs production mode to be roughly doubled, i.e., we find $\mu_F^{(gg+dd)} \simeq 2.3$ in eq. (39). On the other hand, the total Higgs decay width becomes larger due to the new enhanced $h \rightarrow d\bar{d}$ channel, so that the individual Higgs branching ratios are decreased. The net effect is an enhancement in what was previously the gluon-fusion initiated channels and a decrease in the vector-boson initiated signals (μ_{Vjj}). For example, a $\mathcal{O}(50\%)$ enhancement is found in $pp \rightarrow h \rightarrow \tau^+\tau^-$ ($\mu_{F\tau\tau}^{(gg)} \sim 1.5$, see Table IX), partly due to the large $t_\beta \sim 16$ in this model and a $\mathcal{O}(50\%)$ suppression is predicted in this case in the VBF di-photon channel, i.e., $\mu_{V\gamma\gamma}^{(VBF)} \sim 0.5$.

We note that the TRPV Higgs coupling to the d -quarks, λ'_{311} , also contributes to the hV production channel via a t -channel d -quark exchange diagram, $d\bar{d} \rightarrow hV$, and therefore modifies the Higgs production factor in this channel:

$$\mu_V^{(hV+dd)} \equiv \frac{\sigma(q\bar{q} \rightarrow V \rightarrow hV) + \sigma(d\bar{d} \rightarrow hV)}{\sigma(q\bar{q} \rightarrow V \rightarrow hV)_{SM}} = \mu_V^{(hV)} + \frac{\sigma(d\bar{d} \rightarrow hV)}{\sigma(q\bar{q} \rightarrow V \rightarrow hV)_{SM}}, \quad (42)$$

where $\mu_V^{(hV)} = (g_{hVV}^{RPC})^2$ is the hV production factor in the RPC limit and also in our BRPV scenario (since the hVV SUSY coupling is not changed in the BRPV case within the no-VEV basis $\langle v_{\tilde{\nu}} \rangle$, see eq. (23)). Following the above prescription, here also we can define the scaled t -channel hV cross-section via:

$$\sigma(d\bar{d} \rightarrow hV) = (\kappa_d^{TRPV})^2 \cdot \sigma(d\bar{d} \rightarrow hV)_{\kappa_d^{TRPV}=1}, \quad (43)$$

where, using MADGRAPH5_AMC@NLO [145], we find (see also [141]):

$$\frac{\sigma(d\bar{d} \rightarrow hV)_{\kappa_d^{TRPV}=1}}{\sigma(q\bar{q} \rightarrow V \rightarrow hV)_{SM}} \sim 0.05. \quad (44)$$

Thus, the overall change expected in the hV production channel signal due to $\lambda'_{311} \neq 0$ is:

$$\mu_V^{(hV+dd)} \simeq (g_{hVV}^{RPC})^2 + 0.05 \cdot (\kappa_d^{TRPV})^2, \quad (45)$$

which enters only in the $pp \rightarrow hV \rightarrow Vb\bar{b}$ channel, i.e., $\mu_{Vbb}^{(hV)} \rightarrow \mu_{Vbb}^{(hV+dd)}$, and was taken into account in the above analysis, i.e., in Table IX.

Finally, it is also interesting to note that the effect of a new TRPV hdd coupling may also show up in the Higgs pair-production channel $pp \rightarrow hh$, as was suggested in a different context in [141].

TABLE IX: The Higgs observables for the selected benchmark models $\text{BM}\lambda'_{333}$ and $\text{BM}\lambda'_{311}$. See also text.

	$\text{BM}\lambda'_{333}$	$\text{BM}\lambda'_{311}$
$\mu_{F\gamma\gamma}^{(gg)}$	1.26	1.11
$\mu_{FZZ}^{(gg)}$	0.92	1.09
$\mu_{F\tau\tau}^{(gg)}$	0.92	1.09
$\mu_{F\mu\mu}^{(gg)}$	0.93	1.51
$\mu_{V\gamma\gamma}^{(hV)}$	1.04	0.71
$\mu_{V\tau\tau}^{(VBF)}$	1.27	0.48
$\mu_{V\mu\mu}^{(VBF)}$	0.94	0.65

B. The Higgs signals and $\delta_B \cdot \lambda$ RPV effects

When $\lambda_{322} \neq 0$ or $\lambda_{233} \neq 0$, the Higgs decay channels $h \rightarrow \mu^+\mu^-$ or $h \rightarrow \tau^+\tau^-$ are altered, respectively (here also we consider one TRPV coupling at a time). These effects are similar to that depicted in diagram Fig. 2(a), replacing $\lambda' \rightarrow \lambda$ and the outgoing b-quarks with the corresponding leptons. Recall that the TRPV parameters λ_{ijk} are anti-symmetric in their first two indices. We thus restrict ourselves to a one parameter scheme considering one sneutrino type at a time: for the $\lambda_{322} \neq 0$ case we assume BRPV via $\tilde{\nu}_\tau - h$ mixing, whereas when $\lambda_{233} \neq 0$ the BRPV is mediated via $\tilde{\nu}_\mu - h$ mixing. Accordingly, in the $\tilde{\nu}_\tau - h$ mixing BRPV scenario we apply the neutrino mass bound $m_{\nu_\tau} < 18.2$ MeV on the tau-neutrino and in the $\tilde{\nu}_\mu - h$ mixing case we apply the bound $m_{\nu_\mu} < 0.19$ MeV on the muon-neutrino. We do not consider here the possible implications of the λ TRPV couplings on the flavor violating Higgs decay $h \rightarrow \tau\mu$, which was studied in detail in [46].

As in the λ' TRPV case, in the presence of $\lambda_{233} \neq 0$ or $\lambda_{322} \neq 0$, the coupling of the Higgs-sneutrino mixed state to τ 's or muons receives a new TRPV term $\propto \lambda_{233}Z_{h3}$ or $\propto \lambda_{322}Z_{h3}$, respectively (the RPC couplings g_{hl}^{RPC} are defined in eq. (A6)):

$$\Lambda_{h\tau\tau} = g_\tau^{SM} \left(g_{h\tau\tau}^{RPC} + \frac{\lambda_{233}Z_{h3}}{\sqrt{2}g_\tau^{SM}} \right), \quad (46)$$

$$\Lambda_{h\mu\mu} = g_\mu^{SM} \left(g_{h\mu\mu}^{RPC} + \frac{\lambda_{322}Z_{h3}}{\sqrt{2}g_\mu^{SM}} \right), \quad (47)$$

which directly modifies (at tree-level) the Higgs decays $h \rightarrow \tau^+\tau^-$ or $h \rightarrow \mu^+\mu^-$ and also mildly modifies the 1-loop τ or μ exchanges in $h \rightarrow \gamma\gamma$.

In Tables X and XI we list the input parameters and the resulting Higgs signal strength observables for two benchmark models $\text{BM}\lambda_{233}$ and $\text{BM}\lambda_{322}$, setting $\lambda_{233} = 0.7$ or $\lambda_{322} = 0.7$ in the superpotential, which are the (conservative) upper bounds for $m_{\tilde{\tau}_R} > 1$ TeV and $m_{\tilde{\mu}_R} > 1$ TeV, respectively, see [95]. The $\text{BM}\lambda_{233}$ model has been chosen to maximize the TRPV effect in the Higgs decay $h \rightarrow \tau^+\tau^-$, while $\text{BM}\lambda_{322}$ maximizes the TRPV effect in $h \rightarrow \mu^+\mu^-$; both within the 2σ upper bounds on the corresponding Higgs signals, see Table I. In the $\text{BM}\lambda_{322}$ scenario we have also checked that with $\lambda_{322} = 0.7$ the contribution to the muon anomalous magnetic moment, $(g-2)_\mu$, lies within the experimental bound [146], see also [147].

Summarizing our findings and the results in Tables X and XI we find that:

- A better sensitivity to these TRPV couplings via $h \rightarrow \tau^+\tau^-$, $\mu^+\mu^-$ is obtained when the Higgs decay channels to gauginos are kinematically closed, i.e., when the 2nd lightest gauginos are heavier than the lightest Higgs, as is the case in both $\text{BM}\lambda_{233}$ and $\text{BM}\lambda_{322}$ models, see Table XVII.
- As expected, in the $\text{BM}\lambda_{233}$ case the Higgs signals involving τ decays are significantly enhanced by the new TRPV coupling: $\mu_{F\tau\tau}^{(gg)} \sim \mu_{V\tau\tau}^{(VBF)} \sim 1.85$ (we have explicitly checked that the corresponding signal strengths

TABLE X: Input parameters for the selected benchmark models $\text{BM}\lambda_{233}$ and $\text{BM}\lambda_{322}$, with $l = \mu$ and $l = \tau$, respectively, for the parameters $m_{\tilde{\nu}_l}$ and $m_{\tilde{l}_{RR}}$.

	$\text{BM}\lambda_{233}$	$\text{BM}\lambda_{322}$	
δ_ϵ	0	0	
μ	958.82	270.48	[GeV]
M_1	593.21	290.19	[GeV]
M_2	1355.12	1222.63	[GeV]
t_β	4.35	2.72	
δ_B	0.03	0.02	
m_A	2141.48	5007.63	[GeV]
$m_{\tilde{\nu}_l}$	218.16	718.52	[GeV]
$m_{\tilde{q}}$	2591.04	2782.38	[GeV]
\tilde{A}	95.18	1772.84	[GeV]
$m_{\tilde{b}_{RR}}$	4703.45	2381.95	[GeV]
$m_{\tilde{l}_{RR}}$	3133.34	2371.34	[GeV]

in the RPC SUSY limit are close to unity, $\mu_{F\tau\tau,V\tau\tau}(\lambda_{233} = 0) \sim 1$ due to decoupling). This is in contrast to the BRPV scenario $\text{BM}\tau$ with $\delta_\epsilon \sim 0.5$ discussed in the previous section, where the signal strength factors in the $\tau\tau$ -channels were suppressed (see Tables VI-VII). The rest of the Higgs signals in the $\text{BM}\lambda_{233}$ scenario are suppressed with respect to the SM and to the RPC SUSY case. In particular, in the vector-boson Higgs decay channels they saturate their lower 2σ bound, i.e., $\mu_{FZZ}^{(gg)} \sim \mu_{F\mu\mu}^{(gg)} \sim 0.92$ and in the $pp \rightarrow h \rightarrow \mu^+\mu^-$ channel we have $\mu_{F\mu\mu}^{(gg)} \sim 0.94$, primarily due to the enlarged total Higgs decay width thereby decreasing the $BR(h \rightarrow \mu^+\mu^-)$.

- The $\text{BM}\lambda_{322}$ scenario exhibits a large enhancement in the Higgs decay to muons, saturating the upper bound: $\mu_{F\mu\mu}^{(gg)} \sim 1.96$, while keeping the rest of the Higgs signals around unity, which is the value expected in the decoupling RPC SUSY limit and in the SM (we again verified that $\mu_{F\mu\mu}^{(gg)}(\lambda_{322} = 0) \sim 1$, as expected due to decoupling in the RPC SUSY spectrum in this case). Here also the enhanced signal strength in the $h \rightarrow \mu^+\mu^-$ channel is in contrast to the BRPV scenario $\text{BM}\mu$ with $\delta_\epsilon \sim 0.5$, for which we found $\mu_{F\mu\mu}^{(gg)} \sim 0.75$ (see Tables VI-VII).

C. TRPV case - final note

The TRPV benchmark models considered in section V are by no means unique, in the sense that observable TRPV effects in the Higgs signals considered above are possible within a wide range of the SUSY parameter space and, in particular, of the TRPV and BRPV couplings, e.g., with significantly smaller values of the TRPV parameters. To demonstrate that, we consider below the Higgs signal in the $pp \rightarrow h \rightarrow \mu^+\mu^-$ channel, $\mu_{F\mu\mu}^{(gg)}$, within the $\lambda_{322} \neq 0$ TRPV scenario, this time treating λ_{322} as a free parameter in the range $\lambda_{322} \in [0, 0.7]$ and fixing $m_A = 2$ TeV with either $t_\beta = 2$ or $t_\beta = 30$. The rest of the input parameters (apart from the BRPV parameter δ_ϵ which is again set to zero in accordance with the working assumption of section V) are varied in the "standard" ranges given in Table II, i.e., here also the BRPV Higgs-sneutrino mixing parameter, δ_B , is varied in the range $[0, 0.5]$. We again apply all the filters that were used in the previous sections including the 95% CL bound on this channel, i.e., $\mu_{F\mu\mu}^{(gg)} \leq 1.96$ in Table I.

TABLE XI: The Higgs observables for the selected benchmark models $\text{BM}\lambda_{233}$ and $\text{BM}\lambda_{322}$. See also text.

	$\text{BM}\lambda_{233}$	$\text{BM}\lambda_{322}$
$\mu_{F\gamma\gamma}^{(gg)}$	0.94	1.04
$\mu_{FZZ}^{(gg)}$	0.92	0.99
$\mu_{F\tau\tau}^{(gg)}$	1.85	0.99
$\mu_{F\mu\mu}^{(gg)}$	0.94	1.96
$\mu_{Vbb}^{(hV)}$	0.94	1.00
$\mu_{V\gamma\gamma}^{(VBF)}$	0.95	1.05
$\mu_{V\tau\tau}^{(VBF)}$	1.86	1.00

We define the RPV effect as the “distance” from the RPC expectation:

$$\Delta\mu_{F\mu\mu} \equiv \frac{|\mu_{F\mu\mu}^{TRPV} - \mu_{F\mu\mu}^{RPC}|}{\mu_{F\mu\mu}^{RPC}} \quad (48)$$

where $\mu_{F\mu\mu}^{TRPV} \equiv \mu_{F\mu\mu}^{(gg)}(\lambda_{322}, \delta_B)$ and $\mu_{F\mu\mu}^{RPC} = \mu_{F\mu\mu}^{(gg)}(\lambda_{322} = 0, \delta_B = 0)$. We recall again that, since we work in the decoupling SUSY limit, we have $\mu_{F\mu\mu}^{RPC} \simeq \mu_{F\mu\mu}^{SM} \simeq 1$.

In Figs. 3(a), (b) and (c) we give scatter plots in the $\lambda_{322} - \delta_B$ RPV parameter plane, corresponding to RPV SUSY models that pass all the filters and constraints and yield $\Delta\mu_{F\mu\mu} > 0.5, 0.8, 0.95$, respectively. We see for example, that a shift of up to $\mathcal{O}(100\%)$ in the $pp \rightarrow h \rightarrow \mu^+\mu^-$ channel may be generated with values of the TRPV parameter $\lambda_{322} \sim \mathcal{O}(0.1)$, i.e., an order of magnitude smaller than its current upper bounds.

VI. SUMMARY

We have explored the phenomenology of some variations of the RPV SUSY framework, confronting them with recent LHC data on the 125 GeV Higgs production and decay modes and with other available constraints on the RPV parameter space.

We adopt a heavy SUSY scenario with TeV-scale squark and $\text{SU}(2)$ singlet slepton masses as well as the decoupling limit in the SUSY Higgs sector, thereby considering multi-TeV masses for the heavy Higgs states. We then consider a simplified approach for both the Bilinear RPV (BRPV) and Trilinear RPV (TRPV) cases, by assuming non-negligible RPV effects only in a single generation, i.e., BRPV and TRPV interactions involving one sneutrino-flavor at a time, in most cases the 3rd generation sneutrino $\tilde{\nu}_\tau$. We show that the BRPV induced Higgs–sneutrino, lepton–gaugino and charged-Higgs–slepton mixings, give rise to new Higgs decay channels into lepton–gaugino pairs, with possible smoking gun RPV signatures of the form $h \rightarrow \tau^\pm \ell^\mp + \cancel{E}_T$ ($\ell = e, \mu, \tau$), having rates several times larger than the expected SM (see eq. (34)) and/or RPC SUSY rates which are mediated by the Higgs decay $h \rightarrow WW^*$. In some instances, when the SUSY spectrum contains an $\mathcal{O}(100)$ GeV light chargino, these signals are accompanied by an $\mathcal{O}(20 - 30\%)$ enhancement in the di-photon signal $pp \rightarrow h \rightarrow \gamma\gamma$. We also find that detectable BRPV effects of $\mathcal{O}(20 - 30\%)$ might arise in some of the conventional Higgs signals, e.g., in $pp \rightarrow h \rightarrow \mu^+\mu^-, \tau^+\tau^-$ which are unaffected by RPC SUSY effects in the decoupling limit and are, therefore, inherent to the RPV framework.

We further examined TRPV scenarios and found that large RPV effects, in the range of 10–100%, can be generated in several Higgs production and decay modes, if the 125 GeV Higgs-like state is a Higgs-sneutrino BRPV mixed state and the 3rd or 2nd generation sneutrinos have $\mathcal{O}(0.1 - 1)$ TRPV couplings to a pair of muons, τ -leptons and/or to a pair of d or b quarks, i.e., $\tilde{\nu}_\tau\mu\mu, \tilde{\nu}_\mu\tau\tau, \tilde{\nu}_\tau dd$ or $\tilde{\nu}_\tau bb$. In particular, we find that detectable effects in the TRPV scenarios may arise in $pp \rightarrow h \rightarrow \mu^+\mu^-, \tau^+\tau^-$ as well as in $pp \rightarrow Vh \rightarrow Vb\bar{b}$ ($V = W, Z$).

We have provided specific benchmark models for the BRPV and TRPV scenarios and listed the corresponding SUSY parameter space and physical mass spectrum for all the above mentioned BRPV and TRPV effects. In Table XII we

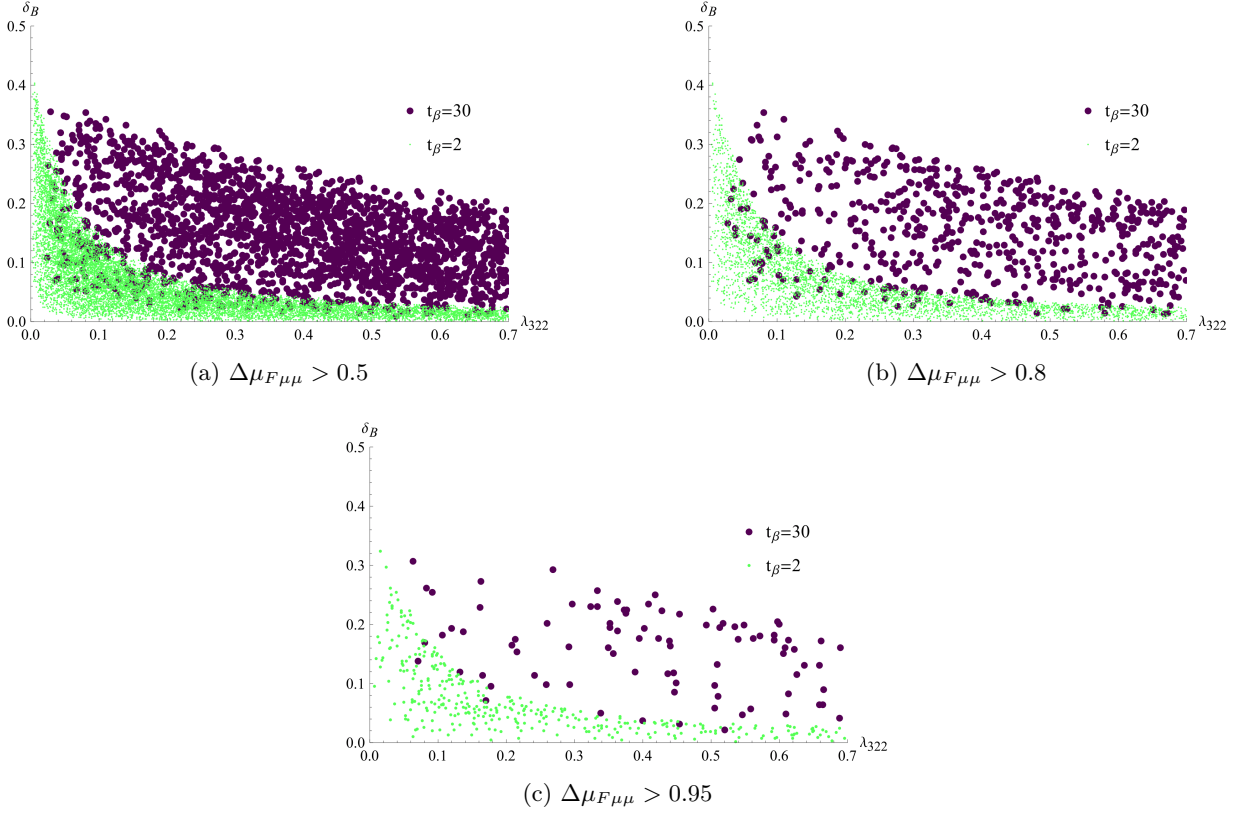


FIG. 3: Scatter-plots in the $\lambda_{322} - \delta_B$ RPV parameter plane, of RPV SUSY models that pass all the filters and constraints and yield $\Delta\mu_{F\mu\mu} > 0.5, 0.8$ and 0.95 , see text and eq. (48).

TABLE XII: Expected RPV effects on the Higgs observables (signal strengths) within the benchmark RPV models considered in the paper.

Decay Mode	Production mode		
	$gg \rightarrow h$	hV	VBF
$h \rightarrow \gamma\gamma$	$\mu_{F\gamma\gamma}^{(gg)} \sim 1.26, \text{ BM}\lambda'_{333}$	-	$\mu_{V\gamma\gamma}^{(VBF)} \sim 0.48, \text{ BM}\lambda'_{311}$
$h \rightarrow ZZ^*$	SM-like	-	-
$h \rightarrow WW^*$	SM-like	-	-
$h \rightarrow b\bar{b}$	-	$\mu_{Vb\bar{b}}^{(hV)} \sim 0.71, \text{ BM}\lambda'_{311}$	-
$h \rightarrow \tau^+\tau^-$	$\mu_{F\tau\tau}^{(gg)} \sim \begin{cases} 0.73, & \text{BM}\tau \\ 1.85, & \text{BM}\lambda_{233} \end{cases}$	-	$\mu_{V\tau\tau}^{(VBF)} \sim \begin{cases} 0.65, & \text{BM}\lambda'_{311} \\ 1.85, & \text{BM}\lambda_{233} \end{cases}$
$h \rightarrow \mu^+\mu^-$	$\mu_{F\mu\mu}^{(gg)} \sim \begin{cases} 0.75, & \text{BM}\mu \\ 1.96, & \text{BM}\lambda_{322} \end{cases}$	-	-

list some of the notable RPV effects on the Higgs signals within these benchmark models.

Appendix A: Higgs couplings, decays and production channels

We list in this appendix part of the relevant analytical expressions for the couplings, decay channels and production mechanisms of the lightest CP-even Higgs-sneutrino mixed state, $h \equiv h_{RPV}$, in our BRPV SUSY framework. The complete set of Feynman rules for the BRPV and TRPV interactions can be found in [75, 87]. In particular, following the notation of [87], we focus below on direct BRPV effects, originating from F-terms, D-terms and from interactions in the superpotential and soft breaking terms, highlighting the analytic features that arise in the BRPV scenario and are relevant to our work.

1. Higgs couplings and decays to heavy vector-bosons

In the no-VEV BRPV basis, $v_{\tilde{\nu}_\tau} = 0$, where the τ -sneutrino doesn't condensate, the hVV couplings ($V = W^\pm, Z$) are left unchanged with respect to the RPC case. That is, as in the RPC case, they scale as $s_{\beta-\alpha} = c_\beta Z_{h1} + s_\beta Z_{h2}$ relative to the corresponding SM coupling strength:

$$\Lambda_{hVV} = g_V^{SM} g_{hVV}^{RPC}, \quad (\text{A1})$$

where $g_Z^{SM} = \frac{1}{2}v(g_1 s_W + g_2 c_W)^2$, $g_W^{SM} = \frac{1}{2}v g_2^2$, $g_{hVV}^{RPC} = c_\beta Z_{h1} + s_\beta Z_{h2}$ and the Higgs mixing elements Z_{h1} and Z_{h2} are determined by the diagonalization of the CP-even Higgs mass-squared matrix m_E^2 (see eq. (11)).

Thus, in our RPV setup the Higgs partial decay width to the vector-bosons as well as the hV and VBF Higgs production channels (which are mediated by the hVV coupling) are also scaled by g_{hVV}^{RPC} [17]:

$$\Gamma(h \rightarrow VV^*) = (g_{hVV}^{RPC})^2 \Gamma_{SM}(h \rightarrow VV^*), \quad (\text{A2})$$

and

$$\sigma(q\bar{q} \rightarrow V \rightarrow hV) = (g_{hVV}^{RPC})^2 \sigma_{SM}(q\bar{q} \rightarrow V \rightarrow hV), \quad (\text{A3})$$

$$\sigma(qq \rightarrow hqq) = (g_{hVV}^{RPC})^2 \sigma_{SM}(qq \rightarrow hqq). \quad (\text{A4})$$

2. Higgs couplings and decays to quarks and leptons

The Higgs couplings to the quarks are also left unchanged with respect to the RPC SUSY case, where they scale relative to the corresponding SM coupling strength as:

$$\Lambda_{hq\bar{q}} = g_q^{SM} g_{hq\bar{q}}^{RPC}, \quad (\text{A5})$$

with $g_q^{SM} = \frac{m_q}{v}$ and $g_{hu\bar{u}}^{RPC} = \frac{Z_{h2}}{s_\beta}$, $g_{hd\bar{d}}^{RPC} = \frac{Z_{h1}}{c_\beta}$, where $u(d)$ stands for an up(down)-quark. As in the RPC case, leptons which do not participate in the BRPV lepton-chargino mixing couple to the Higgs in similar fashion to the down-type quarks:

$$\Lambda_{hl} = g_l^{SM} g_{hl}^{RPC}, \quad (\text{A6})$$

where $g_l^{SM} = \frac{m_l}{v}$ and $g_{hl}^{RPC} = \frac{Z_{h1}}{c_\beta}$. For the Higgs coupling to leptons participating in BRPV lepton-chargino mixing see Appendix A 4.

Thus, the Higgs partial decay width to the a pair of quarks is also scaled with respect to the SM [17]:

$$\Gamma(h \rightarrow q\bar{q}) = (g_{hq\bar{q}}^{RPC})^2 \Gamma_{SM}(h \rightarrow q\bar{q}). \quad (\text{A7})$$

where

$$\Gamma_{SM}(h \rightarrow q\bar{q}) = N_C \frac{G_F m_q^2}{4\sqrt{2}\pi} m_h \left(1 - \frac{4m_q^2}{m_h^2}\right)^{\frac{3}{2}}. \quad (\text{A8})$$

Similar expressions also hold for the Higgs decay to RPC leptons by replacing $q \rightarrow l$ and setting $N_C = 1$. The QCD corrections to eqs. (A8)–(A7) are important and were taken into account in our analysis, using the running masses

evaluated at the scale of the Higgs mass, i.e., $m_q = \overline{m}_q(m_h)$ [17, 148]. In particular, for the b and c quarks we have $\overline{m}_b(m_h) \simeq 2.8$ GeV and $\overline{m}_c(m_h) \simeq 0.6$ GeV, respectively.

3. Higgs couplings to squarks and sleptons

The couplings of the lightest CP-even Higgs-sneutrino mixed state to the squarks and sleptons are relevant in this work for their contributions to the 1-loop decays $h \rightarrow gg$ and $h \rightarrow \gamma\gamma$ and in the calculation of the higher-order corrections to the Higgs mass. We note that the contribution of D-terms to the squark mass matrices is negligible for multi-TeV squarks, as assumed throughout this work.

In the BRPV scenario within the no-VEV basis, the left-right mixing matrices of the up and down-type squarks, Z^U and Z^D , respectively [87], remain unchanged with respect to the RPC case. In particular, the Higgs couplings to the down-type squarks are equal to their values in the RPC case. In particular, there are no new F-terms due to BRPV in the down-squark sector and the BRPV D-terms vanish in the no-VEV basis. Thus, the $h\tilde{b}_i\tilde{b}_j$ coupling is (\tilde{b} is a bottom-squark):¹⁴

$$\Lambda_{h\tilde{b}_i\tilde{b}_j} = \frac{g_2}{m_W} g_{h\tilde{b}_i\tilde{b}_j}^{RPC}, \quad (\text{A9})$$

where we have defined the "reduced" RPC coupling $g_{h\tilde{b}_i\tilde{b}_j}^{RPC}$ and factored out the term $g_2/m_W = 2/v$ for later use (see e.g., [17]). The full expression for $\Lambda_{h\tilde{b}_i\tilde{b}_j}$ can be found in [87].

On the other hand, the Higgs couplings to a pair of up-type squarks do receive a new BRPV F-term contribution which is $\propto y_u \mu \delta_\epsilon Z_{h3}$ (recall that $Z_{h3} = Z_{h3}(\delta_B)$). In particular, for the top-squarks the BRPV F-term can be significant and we have (see also [87]):

$$\Lambda_{h\tilde{t}_i\tilde{t}_j} = \frac{g_2}{m_W} \left(g_{h\tilde{t}_i\tilde{t}_j}^{RPC} - \frac{m_t}{s_\beta} Z_{i1}^U Z_{j2}^U \mu \delta_\epsilon Z_{h3} \right), \quad (\text{A10})$$

where again we factored out the term $g_2/m_W = 2/v$ and introduced the "reduced" RPC coupling $g_{h\tilde{t}_i\tilde{t}_j}^{RPC}$. Note that since Z_{h3} depends on the soft BRPV term δ_B , the new BRPV term in eq. (A10) contains two BRPV insertions, i.e., $\delta_\epsilon \times \delta_B$. It also modifies the contribution of the top-squark loop in the ggh vertex, thereby changing the gluon-fusion Higgs production mode; this effect is taken into account in our analysis.

The BRPV couplings δ_ϵ and δ_B also generate mixing between the charged Higgs states and the charged sleptons. In particular, assuming only a 3rd generation BRPV scenario, the slepton-charged Higgs mass matrix in the $(H_d^-, H_u^+, \tilde{\tau}_L, \tilde{\tau}_R)$ weak basis reads [87]:¹⁵

$$m_{\tilde{\tau}}^2 = \begin{pmatrix} m_W^2 s_\beta^2 + m_A^2 s_\beta^2 & m_W^2 s_\beta c_\beta + \frac{1}{2} m_A^2 s_{2\beta} & -\delta_B s_\beta^2 m_A^2 & -\delta_\epsilon \mu m_\tau t_\beta \\ m_W^2 s_\beta c_\beta + \frac{1}{2} m_A^2 s_{2\beta} & m_W^2 c_\beta^2 + m_A^2 c_\beta^2 & -\frac{1}{2} \delta_B m_A^2 s_{2\beta} & -\delta_\epsilon \mu m_\tau \\ -\delta_B s_\beta^2 m_A^2 & -\frac{1}{2} \delta_B m_A^2 s_{2\beta} & m_\tau^2 + m_{\tilde{\nu}_\tau}^2 - m_W^2 (c_\beta^2 - s_\beta^2) & (A_\tau - \mu t_\beta) m_\tau \\ -\delta_\epsilon \mu m_\tau t_\beta & -\delta_\epsilon \mu m_\tau & (A_\tau - \mu t_\beta) m_\tau & m_\tau^2 + m_{\tilde{\tau}_{RR}}^2 - \frac{1}{4} g_1^2 v (c_\beta^2 - s_\beta^2) \end{pmatrix}, \quad (\text{A11})$$

where $m_{\tilde{\nu}_\tau}^2$ is defined in eq. (12), $m_{\tilde{\tau}_{RR}}^2$ is the right-handed soft mass of the 3rd generation slepton, $\tilde{\tau}$, and we have used the minimization conditions and definitions in eqs. (4)–(9). Also, we have used the MFV relation $A_\tau \propto y_\tau$ by generically setting $A_f \equiv y_f \cdot \tilde{A}$. Note that, as opposed to the squark sector, in the mass matrix $m_{\tilde{\tau}}^2$ of eq. (A11) we have kept the D-terms, since their relative effect is larger in the slepton sector.

The weak states $(H_d^-, H_u^+, \tilde{\tau}_L, \tilde{\tau}_R)$ are given in terms of the physical states $(\tilde{\tau}_j)$ by

$$H_d^- = Z_{j1}^+ \tilde{\tau}_j \quad (\text{A12a})$$

$$H_u^+ = Z_{j2}^+ \tilde{\tau}_j \quad (\text{A12b})$$

$$\tilde{\tau}_L = Z_{j3}^+ \tilde{\tau}_j \quad (\text{A12c})$$

$$\tilde{\tau}_R = Z_{j4}^+ \tilde{\tau}_j \quad (\text{A12d})$$

¹⁴ We note that there is a TRPV F-term in the $h\tilde{b}\tilde{b}$ coupling which is $\propto y_b \lambda'_{333} Z_{h3}$. This term indirectly affects the 1-loop hgg and $h\gamma\gamma$ vertices, but it is negligible for our purpose mainly due to the $1/m_b^2$ suppression in these 1-loop couplings.

¹⁵ In some instances we apply the single generation BRPV working assumption to the 2nd generation, in which case the slepton-charged Higgs mass matrix can be similarly written in the $(H_d^-, H_u^+, \tilde{\mu}_L, \tilde{\mu}_R)$ weak basis and the change in the index $\tau \rightarrow \mu$ should be applied in eq. (A11) in all the relevant entries.

where $\tilde{\tau}_j$ corresponds to the massless Goldstone boson and $\tilde{\tau}_{2,3,4}$ are the physical states which are added in our analysis (e.g., in the 1-loop decay $h \rightarrow \gamma\gamma$) although their effect on the 125 GeV Higgs physics is small in general in the decoupling limit [17].

As mentioned above, the Higgs couplings to the charged sleptons–charged Higgs mixed states are needed for the calculation of the 1-loop $h \rightarrow \gamma\gamma$ decay and for the higher-order corrections to the Higgs mass. These quantities require only the diagonal $h\tilde{\tau}_i\tilde{\tau}_i$ couplings which are given by:

$$\begin{aligned} \Lambda_{h\tilde{\tau}_i\tilde{\tau}_i} = & \frac{g_2}{m_W} \left[g_{h\tilde{\tau}_i\tilde{\tau}_i}^{RPC} - v^2 c_\beta \frac{g_2^2}{4} Z_{i1}^+ Z_{i3}^+ Z_{h3} + \frac{m_\tau}{c_\beta} A_\tau Z_{i1}^+ Z_{i4}^+ Z_{h3} + \frac{m_\tau^2}{c_\beta} Z_{i1}^+ Z_{i3}^+ Z_{h3} + \right. \\ & \left. + \delta_\epsilon \mu \frac{m_\tau}{c_\beta} Z_{i1}^+ Z_{i4}^+ Z_{h2} - v^2 s_\beta \frac{g_2^2}{4} Z_{h3} Z_{i3}^+ Z_{i2}^+ + \mu \frac{m_\tau}{c_\beta} Z_{i4}^+ Z_{h3} Z_{i2}^+ + \delta_\epsilon \mu \frac{m_\tau}{c_\beta} Z_{i4}^+ Z_{h1} Z_{i2}^+ \right], \end{aligned} \quad (\text{A13})$$

where the term $g_2/m_W = 2/v$ is again factored out. We can see from eq. (A13) that the BRPV D-terms ($\propto g_2^2$) correspond to the RPC sneutrino–slepton–charged Higgs and sneutrino–slepton–slepton couplings, and thus depend on the BRPV mixing parameter δ_B through the Z_{h3} rotation. Also, the A_τ term in eq. (A13) originates from the RPC sneutrino–slepton–charged Higgs trilinear coupling. The rest of the terms in eq. (A13) are new BRPV F-terms; the ones that involve the RPC sneutrino depend on δ_B (i.e., through Z_{h3}), while the others are proportional to δ_ϵ .

4. Higgs couplings to Gauginos

The Higgs couplings to the gauginos can be written in a general form as [87]:

$$\Lambda_{h\tilde{\chi}_i^0\tilde{\chi}_j^0/h\chi_i^+\chi_j^-} = \Lambda_{Lij}^{N/C} L + \Lambda_{Rij}^{N/C} R, \quad (\text{A14})$$

where $R(L) = (1 \pm \gamma_5)/2$ and the left and right-handed couplings, $\Lambda_{L/Rij}^{N/C}$ depend on the BRPV parameters δ_ϵ and δ_B . In particular, we have:

$$\Lambda_{R/Lij}^{N/C} \equiv g_{R/Lij}^{N/C(\delta_\epsilon)} + g_{R/Lij}^{N/C(\delta_\epsilon, \delta_B)}, \quad (\text{A15})$$

where $g_{R/Lij}^{N/C(\delta_\epsilon)}$ depend on δ_ϵ and on the elements Z_{h1} and Z_{h2} (which are independent of δ_B), while $g_{R/Lij}^{N/C(\delta_\epsilon, \delta_B)}$ are proportional to the Higgs–sneutrino mixing element Z_{h3} which contain a δ_B insertion. The couplings $g_{R/Lij}^{N/C(\delta_\epsilon, \delta_B)}$ vanish as $\delta_B \rightarrow 0$. Their explicit form is:

$$\text{Neutralinos : } g_{Lij}^{N(\delta_\epsilon, \delta_B)} = g_{Rij}^{N(\delta_\epsilon, \delta_B)} = \frac{1}{2} (g_1 U_{Nj2} U_{Ni1} - g_2 U_{Nj3} U_{Ni1} + i \leftrightarrow j) Z_{h3}, \quad (\text{A16})$$

$$\text{Charginos : } g_{Lij}^{C(\delta_\epsilon, \delta_B)} = \left(\frac{e}{\sqrt{2} s_W} U_{Ri2} U_{Lj1} - \frac{m_\tau}{v c_\beta} U_{Ri1} U_{Lj3} \right) Z_{h3}, \quad (\text{A17})$$

$$g_{Rij}^{C(\delta_\epsilon, \delta_B)} = \left(\frac{e}{\sqrt{2} s_W} U_{Li1} U_{Rj2} - \frac{m_\tau}{v c_\beta} U_{Li3} U_{Rj1} \right) Z_{h3}, \quad (\text{A18})$$

where U_N is the neutralino mixing matrix (see eq. (17)) and $U_{L,R}$ are the chargino mixing matrices (see eq. (18)). The explicit form of the couplings $g_{R/Lij}^{N/C(\delta_\epsilon)}$ are not very enlightening and will not be given here.

In terms of the above couplings, the widths for the decays $h \rightarrow \tilde{\chi}_i^0 \tilde{\chi}_j^0$ and $h \rightarrow \chi_i^+ \chi_j^-$ are given by:

$$\begin{aligned} \Gamma(h \rightarrow \tilde{\chi}_i^0 \tilde{\chi}_j^0 / \chi_i^+ \chi_j^-) = & \left[\left(\left| \Lambda_{Lij}^{N/C} \right|^2 + \left| \Lambda_{Rij}^{N/C} \right|^2 \right) \left(m_h^2 - m_{\tilde{\chi}_i^0/\chi_i^+}^2 - m_{\tilde{\chi}_j^0/\chi_j^-}^2 \right) \right. \\ & \left. - 4 \text{Re} \left\{ \Lambda_{Lij}^{N/C} \Lambda_{Rij}^{N/C} \right\} m_{\tilde{\chi}_i^0/\chi_i^+} m_{\tilde{\chi}_j^0/\chi_j^-} \right] \times \frac{\lambda^{\frac{1}{2}} \left(m_h^2, m_{\tilde{\chi}_i^0/\chi_i^+}^2, m_{\tilde{\chi}_j^0/\chi_j^-}^2 \right)}{16\pi m_h^3}, \end{aligned} \quad (\text{A19})$$

where $i, j = 1 - 5$ for neutralinos and $i, j = 1 - 3$ for the charginos, assuming a single generation BRPV mixing in both sectors. Also, $\lambda(x, y, z) = (x - y - z)^2 - 4yz$ and the gaugino couplings $\Lambda_{L,Rij}^{N/C}$ are defined in eq. (A14) (their full expressions are given in [87]).

We identify the lightest neutralino (RPV) state $\tilde{\chi}_1^0$ as the τ -neutrino, $\nu_\tau \equiv \tilde{\chi}_1^0$, and the lightest chargino as the τ -lepton, $\tau^+ \equiv \tilde{\chi}_1^+$, and we focus in section IV A on the Higgs decays $h \rightarrow \nu_\tau \nu_\tau, \nu_\tau \tilde{\chi}_2^0$ and $h \rightarrow \tau^+ \tau^-, \tau^\pm \tilde{\chi}_2^\mp$, which corresponds to $h \rightarrow \tilde{\chi}_1^0 \tilde{\chi}_1^0, \tilde{\chi}_1^0 \tilde{\chi}_2^0$ and $h \rightarrow \tilde{\chi}_1^+ \tilde{\chi}_1^-, \tilde{\chi}_1^\pm \tilde{\chi}_2^\mp$, respectively. Sample diagrams of the couplings which generate these Higgs decays to a lepton-gaugino pair are given in Figs. 4 and 5.

We also note the following:

- The $h\tau^+\tilde{\chi}_2^-$ as well as the $h\nu_\tau\nu_\tau$ (for $m_{\nu_\tau} \rightarrow 0$) and $h\nu_\tau\tilde{\chi}_2^0$ couplings have no RPC equivalent and are, therefore, pure RPV couplings.
- The $h\tau^+\tilde{\chi}_2^-$ and $h\nu_\tau\tilde{\chi}_2^0$ RPV couplings have a term proportional only to $Z_{h3} = Z_{h3}(\delta_B)$ (see eqs. (A16) and (A18)). These terms are new BRPV D-terms which are generated from the RPC sneutrino–Wino/Higgsino– τ and sneutrino–Zino–neutrino interactions, respectively, due to the $\tilde{\nu}_\tau - h$ mixing effect.
- Both $h\tau^+\tilde{\chi}_2^-$ and $h\nu_\tau\tilde{\chi}_2^0$ RPV couplings also have a pure BRPV contribution from the superpotential, which depend only on δ_ϵ (see diagrams Fig. 4(c) and Fig. 5(c)).
- The RPV coupling of a Higgs to a pair of τ -neutrinos $\Lambda_{h\nu_\tau\nu_\tau}$ (which in the RPC limit vanish for $m_{\nu_\tau} \rightarrow 0$) contains two BRPV insertions, being proportional to either δ_ϵ^2 or to $\delta_\epsilon \cdot \delta_B$. This coupling is, therefore, suppressed with respect to $\Lambda_{h\nu_\tau\tilde{\chi}_2^0}$, which as mentioned above, can be generated with a single BRPV insertion. Indeed, this is verified in our numerical simulations where we find that $h \rightarrow \nu_\tau \nu_\tau$ is suppressed by several orders of magnitude compared to $h \rightarrow \nu_\tau \tilde{\chi}_2^0$ (i.e., when $m_{\tilde{\chi}_2^0} < m_h$).

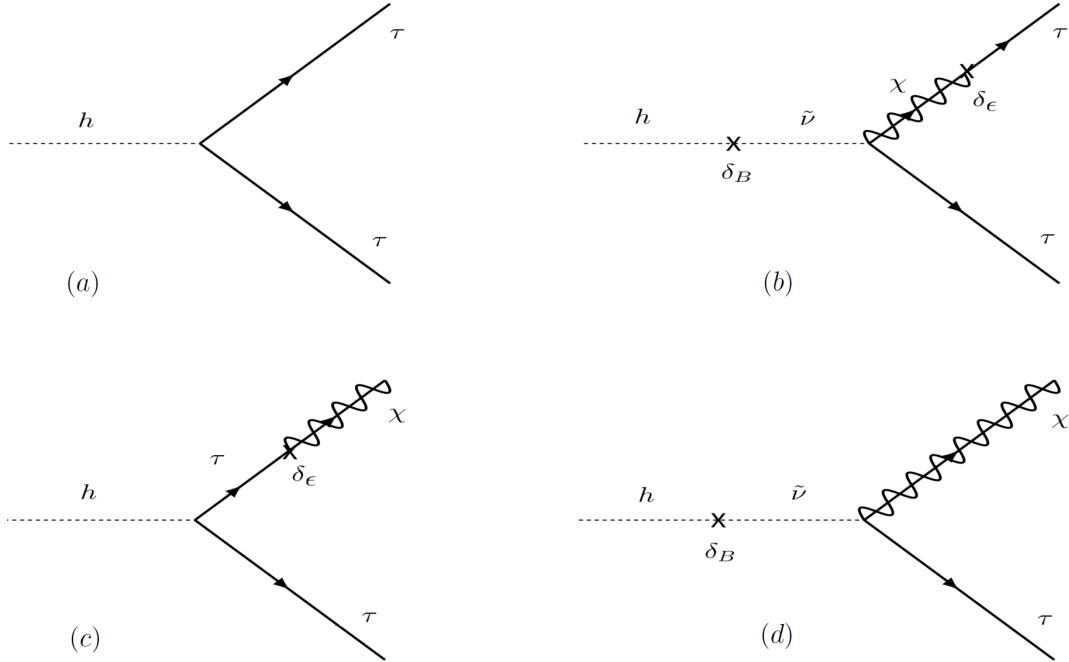


FIG. 4: Sample diagrams of the Higgs couplings/decays $h \rightarrow \tau^+ \tau^-$ (diagrams (a) and (b)) and $h \rightarrow \tau^\pm \tilde{\chi}^\mp$ (diagrams (c) and (d)).

5. The 1-loop decay $h \rightarrow \gamma\gamma$

The Higgs decay to a pair of photons in the SM is given by [148]:

$$\Gamma_{SM}(h \rightarrow \gamma\gamma) = \frac{G_F \alpha^2 m_h^3}{128 \sqrt{2} \pi^3} \left| \sum_f N_C Q_f^2 A_{\frac{1}{2}}(\tau_f) + A_1(\tau_W) \right|^2 \quad (\text{A20})$$

where $\tau_i = \frac{4m_i^2}{m_h^2}$ and the expressions for the loop functions $A_{\frac{1}{2}}$ (for a fermion loop) and A_1 (for the W loop) can be found in [148]. The dominant SM contributions arise from the top-quark and W -boson loop exchanges.

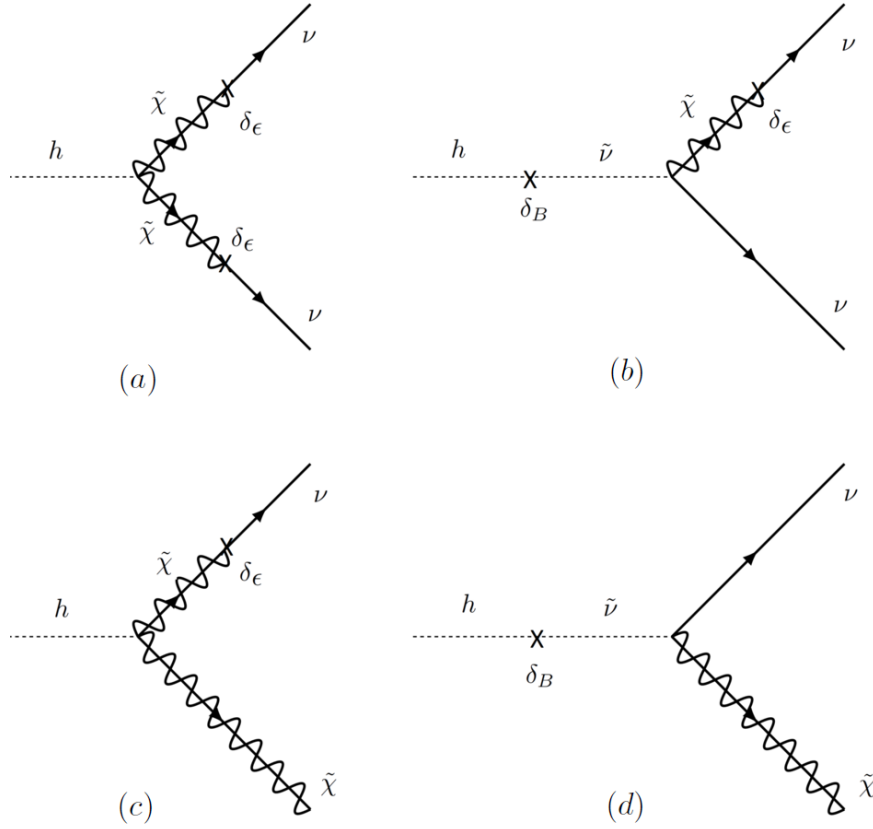


FIG. 5: Diagrammatic description of the Higgs couplings/decays $h \rightarrow \nu_\tau \nu_\tau$ (diagrams (a) and (b)) and $h \rightarrow \nu_\tau \tilde{\chi}^0$ (diagrams (c) and (d)).

In the BRPV SUSY framework, the Higgs decay to a pair of photons can be cast in the following form [17]:

$$\begin{aligned}
 \Gamma(h \rightarrow \gamma\gamma) = & \\
 & \frac{G_F \alpha^2 m_h^3}{128 \sqrt{2} \pi^3} \times \left[\sum_{q=t,b} N_C Q_f^2 g_{hq\bar{q}}^{RPC} A_{\frac{1}{2}}(\tau_q) + g_{hVV}^{RPC} A_1(\tau_W) \right. \\
 & + \sum_{i=1}^3 \frac{2m_W}{m_{\chi_i^\pm}} \frac{\Lambda_{ii}^C}{e} A_{\frac{1}{2}}(\tau_{\chi_i^\pm}) \\
 & + \frac{v}{2} \sum_{i=1}^2 \left[\frac{\Lambda_{h\tilde{b}_i\tilde{b}_i}}{m_{\tilde{b}_i}^2} N_C Q_b^2 A_0(\tau_{\tilde{b}_i}) + \frac{\Lambda_{h\tilde{t}_i\tilde{t}_i}}{m_{\tilde{t}_i}^2} N_C Q_t^2 A_0(\tau_{\tilde{t}_i}) \right] \\
 & \left. + \frac{v}{2} \sum_{i=2}^4 \frac{\Lambda_{h\tilde{\tau}_i\tilde{\tau}_i}}{m_{\tilde{\tau}_i}^2} A_0(\tau_{\tilde{\tau}_i}) \right]^2 \tag{A21}
 \end{aligned}$$

where $\Lambda_{ii}^C = \Lambda_{Lii}^C = \Lambda_{Rii}^C$ and $\Lambda_{h\tilde{f}_i\tilde{f}_i}$ ($f = \tau, b, t$) are the diagonal Higgs couplings to the charginos and sfermions which are defined above.

We note that, for the heavy sfermion spectrum that is considered in this work, the chargino contributions to $h \rightarrow \gamma\gamma$ are much larger than the sfermions one.

6. The 1-loop decay $h \rightarrow gg$

In the SM, the loop-induced Higgs decay to a pair of gluons is given by [148]:

$$\Gamma_{SM}(h \rightarrow gg) = K_{SM}^{QCD} \frac{G_F \alpha_s^2 m_h^3}{36\sqrt{2}\pi^3} \left| \frac{3}{4} \sum_{q=t,b} A_{\frac{1}{2}}(\tau_q) \right|^2, \quad (\text{A22})$$

where the QCD corrections to eq. (A22) are taken into account by the QCD K-factor and by using the quark running masses evaluated at the scale of the Higgs mass: $m_q = \bar{m}_q(m_h)$ [148]. In particular, the SM QCD K-factor is $K_{SM}^{QCD} \simeq 1.84$ and $\bar{m}_b(m_h) \simeq 2.8$ GeV, $\bar{m}_c(m_h) \simeq 0.6$ GeV.

In the BRPV SUSY framework, the loop-induced $h \rightarrow gg$ amplitude receives additional contributions from the squarks; the dominant ones are generated by the sbottoms and stops [17]:

$$\begin{aligned} \Gamma(h \rightarrow gg) = K^{QCD} \frac{G_F \alpha_s^2 m_h^3}{36\sqrt{2}\pi^3} \times & \left| \frac{3}{4} \sum_{q=t,b} g_{hq\bar{q}}^{RPC} A_{\frac{1}{2}}(\tau_q) \right. \\ & \left. + \frac{3v}{8} \sum_{i=1}^2 \left[\frac{\Lambda_{h\bar{b}_i\bar{b}_i}}{m_{\bar{b}_i}^2} A_0(\tau_{\bar{b}_i}) + \frac{\Lambda_{h\bar{t}_i\bar{t}_i}}{m_{\bar{t}_i}^2} A_0(\tau_{\bar{t}_i}) \right] \right|^2. \end{aligned} \quad (\text{A23})$$

In the decoupling limit the squarks contribution is subdominant and, since in this limit we also have to a good approximation $K^{QCD} \simeq K_{SM}^{QCD}$ [17], we expect a small deviation in $\Gamma(h \rightarrow gg)$ compared to the corresponding RPC SUSY rate and, therefore, also a small deviation in the gluon-fusion Higgs production mechanism.

Appendix B: RPV SUSY Spectra of the benchmark models

In this appendix we list the SUSY spectrum for each of the benchmark models in sections IV–V. The SUSY spectrum of the BRPV benchmark models BM1A-BM1B, BM2-BM3 and BM μ -BM τ are given in Tables XIII, XIV and XV, respectively, and the SUSY spectrum of the TRPV benchmark models BM λ'_{333} -BM λ'_{311} and BM λ_{233} -BM λ_{322} are given in Tables XVI and XVII, respectively.

TABLE XIII: SUSY mass spectrum corresponding to the benchmark models BM1A and BM1B. We have denoted by $\tilde{\chi}_i^0$ the neutralino states, by χ_i^\pm the chargino states, $(\tilde{\nu}_\tau^E, H)$ are the CP-even sneutrino and heavy Higgs states, respectively and $(\tilde{\nu}_\tau^O, A)$ are the CP-odd sneutrino and pseudoscalar Higgs, respectively. Also, $\tilde{\tau}_i$ are the slepton states, \tilde{t}_i are the stops and \tilde{b}_i are the sbottom states. All masses are given in GeV.

	BM1A	BM1B
$(\tilde{\chi}_2^0, \tilde{\chi}_3^0, \tilde{\chi}_4^0, \tilde{\chi}_5^0)$	(94.2, 510.4, 628.3, 650.7)	(90.1, 97.6, 1034.6, 2031.4)
(χ_2^\pm, χ_3^\pm)	(94.3, 638.7)	(91.9, 1034.6)
$(\tilde{\nu}_\tau^E, H)$	(200.2, 4473.6)	(162.8, 2574.3)
$(\tilde{\nu}_\tau^O, A)$	(200.1, 4472.8)	(162.4, 2573.4)
$(\tilde{\tau}_2, \tilde{\tau}_3, \tilde{\tau}_4)$	(210.2, 1509.2, 4473.5)	(176.8, 1303.9, 2574.6)
$(\tilde{t}_1, \tilde{t}_2)$	(6056.3, 6091.8)	(2779.5, 2949.3)
$(\tilde{b}_1, \tilde{b}_2)$	(4814.4, 6071.6)	(2860.5, 4996.4)

TABLE XIV: SUSY mass spectrum corresponding to the benchmark models BM2 and BM3. See also caption to Table XIII.

	BM2	BM3
$(\tilde{\chi}_2^0, \tilde{\chi}_3^0, \tilde{\chi}_4^0, \tilde{\chi}_5^0)$	(93.5, 223.7, 227.6, 999.2)	(86.0, 125.9, 163.6, 1006.2)
(χ_2^\pm, χ_3^\pm)	(215.9, 999.2)	(118.6, 1006.3)
$(\tilde{\nu}_\tau^E, H)$	(229.8, 2748.4)	(163.2, 3179.2)
$(\tilde{\nu}_\tau^O, A)$	(229.5, 2747.6)	(163.0, 3178.7)
$(\tilde{\tau}_2, \tilde{\tau}_3, \tilde{\tau}_4)$	(240.1, 1122.6, 2748.7)	(178.3, 2670.4, 3179.7)
$(\tilde{t}_1, \tilde{t}_2)$	(4631.2, 4631.7)	(826.2, 1330.9)
$(\tilde{b}_1, \tilde{b}_2)$	(4245.0, 4628.2)	(1094.0, 4721.6)

ACKNOWLEDGMENTS

The work of AS was supported in part by the U.S. DOE contract #de-sc0012704. JC would like to thank Tal Miller for his assistance in the numerical sessions.

TABLE XV: SUSY mass spectrum corresponding to the benchmark models $\text{BM}\mu$ and $\text{BM}\tau$. For the states $\tilde{\nu}_l^E$, $\tilde{\nu}_l^O$ and \tilde{l}_i we have $l = \mu$ in the $\text{BM}\mu$ model and $l = \tau$ in $\text{BM}\tau$. See also caption to Table XIII.

	$\text{BM}\mu$	$\text{BM}\tau$
$(\tilde{\chi}_2^0, \tilde{\chi}_3^0, \tilde{\chi}_4^0, \tilde{\chi}_5^0)$	(632.2, 713.1, 761.7, 1428.1)	(633.1, 707.0, 760.1, 1653.1)
(χ_2^\pm, χ_3^\pm)	(633.2, 764.0)	(634.1, 762.0)
$(\tilde{\nu}_l^E, H)$	(181.3, 8996.4)	(174.8, 8545.1)
$(\tilde{\nu}_l^O, A)$	(181.3, 8996.4)	(174.8, 8545.0)
$(\tilde{l}_2, \tilde{l}_3, \tilde{l}_4)$	(197.4, 4249.4, 8996.7)	(191.5, 4145.2, 8545.4)
$(\tilde{t}_1, \tilde{t}_2)$	(2201.0, 2233.7)	(2416.1, 2427.2)
$(\tilde{b}_1, \tilde{b}_2)$	(2210.7, 4720.7)	(2415.5, 4594.0)

TABLE XVI: SUSY mass spectrum corresponding to the benchmark models $\text{BM}\lambda'_{333}$ and $\text{BM}\lambda'_{311}$. See also caption to Table XIII.

	$\text{BM}\lambda'_{333}$	$\text{BM}\lambda'_{311}$
$(\tilde{\chi}_2^0, \tilde{\chi}_3^0, \tilde{\chi}_4^0, \tilde{\chi}_5^0)$	(150.2, 205.4, 303.5, 762.9)	(552.0, 558.0, 1594.1, 1749.2)
(χ_2^\pm, χ_3^\pm)	(153.1, 305.9)	(554.2, 1594.2)
$(\tilde{\nu}_\tau^E, H)$	(725.7, 2166.1)	(203.2, 1661.2)
$(\tilde{\nu}_\tau^O, A)$	(725.7, 2165.0)	(203.1, 1661.1)
$(\tilde{\tau}_2, \tilde{\tau}_3, \tilde{\tau}_4)$	(729.1, 2166.5, 2357.4)	(218.2, 1663.0, 3693.5)
$(\tilde{t}_1, \tilde{t}_2)$	(3443.2, 3487.3)	(2014.4, 2017.0)
$(\tilde{b}_1, \tilde{b}_2)$	(2764.4, 3461.0)	(2008.1, 2421.6)

TABLE XVII: SUSY mass spectrum corresponding to the benchmark models $\text{BM}\lambda_{233}$ and $\text{BM}\lambda_{322}$. For the states $\tilde{\nu}_l^E$, $\tilde{\nu}_l^O$ and \tilde{l}_i we have $l = \mu$ in the $\text{BM}\lambda_{233}$ model and $l = \tau$ in $\text{BM}\lambda_{322}$. See also caption to Table XIII.

	$\text{BM}\lambda_{233}$	$\text{BM}\lambda_{322}$
$(\chi_2^0, \chi_3^0, \chi_4^0, \chi_5^0)$	(589.7, 951.3, 959.9, 1367.1)	(236.3, 271.8, 319.4, 1228.8)
(χ_2^\pm, χ_3^\pm)	(948.3, 1367.1)	(265.7, 1228.8)
$(\tilde{\nu}_l^E, H)$	(207.5, 2143.0)	(709.3, 5009.4)
$(\tilde{\nu}_l^O, A)$	(207.5, 2142.5)	(709.3, 5008.9)
$(\tilde{l}_2, \tilde{l}_3, \tilde{l}_4)$	(220.9, 2144.0, 3133.3)	(712.7, 2371.3, 5009.5)
$(\tilde{t}_1, \tilde{t}_2)$	(2592.6, 2600.9)	(2735.2, 2839.2)
$(\tilde{b}_1, \tilde{b}_2)$	(2591.0, 4703.4)	(2381.9, 2782.3)

-
- [1] Georges Aad et al. Observation of a new particle in the search for the Standard Model Higgs boson with the ATLAS detector at the LHC. *Phys. Lett.*, B716:1–29, 2012, 1207.7214.
- [2] Serguei Chatrchyan et al. Observation of a new boson at a mass of 125 GeV with the CMS experiment at the LHC. *Phys. Lett.*, B716:30–61, 2012, 1207.7235.
- [3] Morad Aaboud et al. Observation of $H \rightarrow b\bar{b}$ decays and VH production with the ATLAS detector. *Phys. Lett.*, B786:59–86, 2018, 1808.08238.
- [4] A. M. Sirunyan et al. Observation of Higgs boson decay to bottom quarks. *Phys. Rev. Lett.*, 121(12):121801, 2018, 1808.08242.
- [5] Morad Aaboud et al. Measurements of gluon-gluon fusion and vector-boson fusion Higgs boson production cross-sections in the $H \rightarrow WW^* \rightarrow e\nu\mu\nu$ decay channel in pp collisions at $\sqrt{s} = 13$ TeV with the ATLAS detector. 2018, 1808.09054.
- [6] Albert M. Sirunyan et al. Measurements of properties of the Higgs boson decaying to a W boson pair in pp collisions at $\sqrt{s} = 13$ TeV. *Submitted to: Phys. Lett.*, 2018, 1806.05246.
- [7] The ATLAS Collaboration. Measurements of the Higgs boson production, fiducial and differential cross sections in the 4ℓ decay channel at $\sqrt{s} = 13$ TeV with the ATLAS detector. 2018.
- [8] CMS Collaboration. Measurements of properties of the Higgs boson in the four-lepton final state at $\sqrt{s} = 13$ TeV. 2018.
- [9] The ATLAS Collaboration. Measurements of Higgs boson properties in the diphoton decay channel using 80 fb^{-1} of pp collision data at $\sqrt{s} = 13$ TeV with the ATLAS detector. 2018.
- [10] Albert M Sirunyan et al. Measurements of Higgs boson properties in the diphoton decay channel in proton-proton collisions at $\sqrt{s} = 13$ TeV. 2018, 1804.02716.
- [11] The ATLAS Collaboration. Cross-section measurements of the Higgs boson decaying to a pair of tau leptons in proton-proton collisions at $\sqrt{s} = 13$ TeV with the ATLAS detector. 2018.
- [12] CMS Collaboration. Search for the standard model Higgs boson decaying to a pair of τ leptons and produced in association with a W or a Z boson in proton-proton collisions at $\sqrt{s} = 13$ TeV. 2018.
- [13] The ATLAS collaboration. A search for the rare decay of the Standard Model Higgs boson to dimuons in pp collisions at $\sqrt{s} = 13$ TeV with the ATLAS Detector. 2018.
- [14] Albert M. Sirunyan et al. Search for the Higgs boson decaying to two muons in proton-proton collisions at $\sqrt{s} = 13$ TeV. *Phys. Rev. Lett.*, 122(2):021801, 2019, 1807.06325.
- [15] Stephen P. Martin. A Supersymmetry primer. pages 1–98, 1997, hep-ph/9709356. [Adv. Ser. Direct. High Energy Phys.18,1(1998)].
- [16] Mikolaj Misiak, Stefan Pokorski, and Janusz Rosiek. Supersymmetry and FCNC effects. *Adv. Ser. Direct. High Energy Phys.*, 15:795–828, 1998, hep-ph/9703442. [,795(1997)].
- [17] Abdelhak Djouadi. The Anatomy of electro-weak symmetry breaking. II. The Higgs bosons in the minimal supersymmetric model. *Phys. Rept.*, 459:1–241, 2008, hep-ph/0503173.
- [18] Howard Georgi and David B. Kaplan. Composite Higgs and Custodial SU(2). *Phys. Lett.*, 145B:216–220, 1984.
- [19] Roberto Contino, Margherita Ghezzi, Christophe Grojean, Margarete Muhlleitner, and Michael Spira. Effective Lagrangian for a light Higgs-like scalar. *JHEP*, 07:035, 2013, 1303.3876.
- [20] Vernon Barger, Paul Langacker, Mathew McCaskey, Michael J. Ramsey-Musolf, and Gabe Shaughnessy. LHC Phenomenology of an Extended Standard Model with a Real Scalar Singlet. *Phys. Rev.*, D77:035005, 2008, 0706.4311.
- [21] Laura Lopez-Honorez, Thomas Schwetz, and Jure Zupan. Higgs portal, fermionic dark matter, and a Standard Model like Higgs at 125 GeV. *Phys. Lett.*, B716:179–185, 2012, 1203.2064.
- [22] Christoph Englert, Tilman Plehn, Dirk Zerwas, and Peter M. Zerwas. Exploring the Higgs portal. *Phys. Lett.*, B703:298–305, 2011, 1106.3097.
- [23] Abdelhak Djouadi, Adam Falkowski, Yann Mambrini, and Jeremie Quevillon. Direct Detection of Higgs-Portal Dark Matter at the LHC. *Eur. Phys. J.*, C73(6):2455, 2013, 1205.3169.
- [24] Sarah Andreas, Chiara Arina, Thomas Hambye, Fu-Sin Ling, and Michel H. G. Tytgat. A light scalar WIMP through the Higgs portal and CoGeNT. *Phys. Rev.*, D82:043522, 2010, 1003.2595.
- [25] R. Barbier et al. R-parity violating supersymmetry. *Phys. Rept.*, 420:1–202, 2005, hep-ph/0406039.
- [26] Yuval Grossman and Howard E. Haber. (S)neutrino properties in R-parity violating supersymmetry. 1. CP conserving phenomena. *Phys. Rev.*, D59:093008, 1999, hep-ph/9810536.
- [27] Yuval Grossman and Howard E. Haber. Neutrino masses and sneutrino mixing in R-parity violating supersymmetry. 1999, hep-ph/9906310.
- [28] M. Hirsch, M. A. Diaz, W. Porod, J. C. Romao, and J. W. F. Valle. Neutrino masses and mixings from supersymmetry with bilinear R parity violation: A Theory for solar and atmospheric neutrino oscillations. *Phys. Rev.*, D62:113008, 2000, hep-ph/0004115. [Erratum: Phys. Rev.D65,119901(2002)].
- [29] M. A. Diaz, M. Hirsch, W. Porod, J. C. Romao, and J. W. F. Valle. Solar neutrino masses and mixing from bilinear R parity broken supersymmetry: Analytical versus numerical results. *Phys. Rev.*, D68:013009, 2003, hep-ph/0302021. [Erratum: Phys. Rev.D71,059904(2005)].
- [30] Sacha Davidson and Marta Losada. Neutrino masses in the R(p) violating MSSM. *JHEP*, 05:021, 2000, hep-ph/0005080.
- [31] Asmaa Abada, Sacha Davidson, and Marta Losada. Neutrino masses and mixings in the MSSM with soft bilinear R(p) violation. *Phys. Rev.*, D65:075010, 2002, hep-ph/0111332.

- [32] Yuval Grossman and Subhendu Rakshit. Neutrino masses in R-parity violating supersymmetric models. *Phys. Rev.*, D69:093002, 2004, hep-ph/0311310.
- [33] M. Hirsch and J. W. F. Valle. Supersymmetric origin of neutrino mass. *New J. Phys.*, 6:76, 2004, hep-ph/0405015.
- [34] Subhendu Rakshit. Neutrino masses and R-parity violation. *Mod. Phys. Lett.*, A19:2239–2258, 2004, hep-ph/0406168.
- [35] Yuval Grossman and Clara Peset. Neutrino masses in RPV models with two pairs of Higgs doublets. *JHEP*, 04:033, 2014, 1401.1818.
- [36] Roshni Bose, Amitava Datta, Anirban Kundu, and Sujoy Poddar. LHC signatures of neutrino mass generation through R-parity violation. *Phys. Rev.*, D90(3):035007, 2014, 1405.1282.
- [37] M. Hanussek and J. S. Kim. Testing neutrino masses in the R-parity violating minimal supersymmetric standard model with LHC results. *Phys. Rev.*, D85:115021, 2012, 1205.0019.
- [38] A. Santamaria and J. W. F. Valle. Spontaneous R-Parity Violation in Supersymmetry: A Model for Solar Neutrino Oscillations. *Phys. Lett.*, B195:423–428, 1987.
- [39] Asmaa Abada and Gregory Moreau. An Origin for small neutrino masses in the NMSSM. *JHEP*, 08:044, 2006, hep-ph/0604216.
- [40] E. J. Chun, S. K. Kang, C. W. Kim, and U. W. Lee. Supersymmetric neutrino masses and mixing with R-parity violation. *Nucl. Phys.*, B544:89–103, 1999, hep-ph/9807327.
- [41] J. M. Mira, E. Nardi, D. A. Restrepo, and J. W. F. Valle. Bilinear R-parity violation and small neutrino masses: A Selfconsistent framework. *Phys. Lett.*, B492:81–90, 2000, hep-ph/0007266.
- [42] F. de Campos, M. A. Garcia-Jareno, Anjan S. Joshipura, J. Rosiek, and J. W. F. Valle. Novel scalar boson decays in SUSY with broken r parity. *Nucl. Phys.*, B451:3–15, 1995, hep-ph/9502237.
- [43] J. Rosiek. Effects of R-parity breaking in the Higgs sector. In *Elementary particle physics: Present and future. Proceedings, International Workshop, Valencia, Spain, June 5-9, 1995*, pages 0295–301, 1995, hep-ph/9508355.
- [44] A. Dedes, S. Rimmer, J. Rosiek, and M. Schmidt-Sommerfeld. On the neutral scalar sector of the general R-parity violating MSSM. *Phys. Lett.*, B627:161–173, 2005, hep-ph/0506209.
- [45] D. Aristizabal Sierra, W. Porod, D. Restrepo, and Carlos E. Yaguna. Novel Higgs decay signals in R-parity violating models. *Phys. Rev.*, D78:015015, 2008, 0804.1907.
- [46] Abdesslam Arhrib, Yifan Cheng, and Otto C. W. Kong. Comprehensive analysis on lepton flavor violating Higgs boson to $\mu^\mp \tau^\pm$ decay in supersymmetry without R parity. *Phys. Rev.*, D87(1):015025, 2013, 1210.8241.
- [47] Raghavendra Srikanth Hundi. Implications of Higgs boson to diphoton decay rate in the bilinear R-parity violating supersymmetric model. *Phys. Rev.*, D87(11):115005, 2013, 1303.4583.
- [48] Herbi K. Dreiner, Kilian Nickel, and Florian Staub. On the two-loop corrections to the Higgs mass in trilinear R-parity violation. *Phys. Lett.*, B742:261–265, 2015, 1411.3731.
- [49] Sanjoy Biswas, Eung Jin Chun, and Pankaj Sharma. Di-Higgs signatures from R-parity violating supersymmetry as the origin of neutrino mass. *JHEP*, 12:062, 2016, 1604.02821.
- [50] Chao-Hsi Chang, Tai-Fu Feng, Yu-Li Yan, Hai-Bin Zhang, and Shu-Min Zhao. Spontaneous R -parity violation in the minimal gauged (B-L) supersymmetry with a 125 GeV Higgs boson. *Phys. Rev.*, D90(3):035013, 2014, 1401.4586.
- [51] Katri Huitu and Harri Waltari. Higgs sector in NMSSM with right-handed neutrinos and spontaneous R-parity violation. *JHEP*, 11:053, 2014, 1405.5330.
- [52] Priyotosh Bandyopadhyay, Pradipta Ghosh, and Sourov Roy. Unusual Higgs boson signal in R-parity violating nonminimal supersymmetric models at the LHC. *Phys. Rev.*, D84:115022, 2011, 1012.5762.
- [53] Anindya Datta, Partha Konar, and Biswarup Mukhopadhyaya. New Higgs signals from vector boson fusion in R-parity violating supersymmetry. *Phys. Rev.*, D63:095009, 2001, hep-ph/0009112.
- [54] Christopher Brust, Andrey Katz, Scott Lawrence, and Raman Sundrum. SUSY, the Third Generation and the LHC. *JHEP*, 03:103, 2012, 1110.6670.
- [55] Wolfgang Altmannshofer, P. S. Bhupal Dev, and Amarjit Soni. $R_{D^{(*)}}$ anomaly: A possible hint for natural supersymmetry with R-parity violation. *Phys. Rev.*, D96(9):095010, 2017, 1704.06659.
- [56] N. G. Deshpande and Xiao-Gang He. Consequences of R-parity violating interactions for anomalies in $\bar{B} \rightarrow D^{(*)} \tau \bar{\nu}$ and $b \rightarrow s \mu^+ \mu^-$. *Eur. Phys. J.*, C77(2):134, 2017, 1608.04817.
- [57] Diganta Das, Chandan Hati, Girish Kumar, and Namit Mahajan. Scrutinizing R-parity violating interactions in light of $R_{K^{(*)}}$ data. *Phys. Rev.*, D96(9):095033, 2017, 1705.09188.
- [58] Kevin Earl and Thomas Gr aigoire. Contributions to $b \rightarrow s \ell \ell$ Anomalies from R-Parity Violating Interactions. *JHEP*, 08:201, 2018, 1806.01343.
- [59] Andreas Redelbach. Searches for Prompt R-Parity-Violating Supersymmetry at the LHC. *Adv. High Energy Phys.*, 2015:982167, 2015, 1512.05956.
- [60] Daniel Dercks, Herbi Dreiner, Manuel E. Krauss, Toby Opferkuch, and Annika Reimert. R-Parity Violation at the LHC. *Eur. Phys. J.*, C77(12):856, 2017, 1706.09418.
- [61] Nils-Erik Bomark, A. Kvellestad, S. Lola, P. Osland, and A. R. Raklev. R-parity violating chargino decays at the LHC. *JHEP*, 12:121, 2014, 1410.0921.
- [62] Sebastian Dumitru, Burt A. Ovrut, and Austin Purves. R-parity Violating Decays of Wino Chargino and Wino Neutralino LSPs and NLSPs at the LHC. 2018, 1811.05581.
- [63] Csaba Csaki, Eric Kuflik, Salvator Lombardo, Oren Slone, and Tomer Volansky. Phenomenology of a Long-Lived LSP with R-Parity Violation. *JHEP*, 08:016, 2015, 1505.00784.

- [64] Joshua Berger, Maxim Perelstein, Michael Saelim, and Philip Tanedo. The Same-Sign Dilepton Signature of RPV/MFV SUSY. *JHEP*, 04:077, 2013, 1302.2146.
- [65] Peter W. Graham, Surjeet Rajendran, and Prashant Saraswat. Supersymmetric crevices: Missing signatures of R-parity violation at the LHC. *Phys. Rev.*, D90(7):075005, 2014, 1403.7197.
- [66] Nosiphiwo Zwane. Long-Lived Particle Searches in R-Parity Violating MSSM. *J. Phys.*, G44(10):105003, 2017, 1505.03479.
- [67] S. Bar-Shalom, G. Eilam, and B. Mele. Sneutrino-Higgs mixing in W W and Z Z production in supersymmetry with R-parity violation. *Phys. Lett.*, B500:297–303, 2001, hep-ph/0005295.
- [68] S. Bar-Shalom, G. Eilam, and B. Mele. New scalar resonances from sneutrino Higgs mixing in supersymmetry with small lepton number (R-parity) violation. *Phys. Rev.*, D64:095008, 2001, hep-ph/0106053.
- [69] Janusz Rosiek. Complete Set of Feynman Rules for the Minimal Supersymmetric Extension of the Standard Model. *Phys. Rev.*, D41:3464, 1990.
- [70] D. P. Roy. R-parity violating SUSY model. *Pramana*, 41:S333–S346, 1993, hep-ph/9303324.
- [71] Gautam Bhattacharyya. R-parity violating supersymmetric Yukawa couplings: A Minireview. *Nucl. Phys. Proc. Suppl.*, 52A:83–88, 1997, hep-ph/9608415.
- [72] Herbert K. Dreiner. An Introduction to explicit R-parity violation. pages 462–479, 1997, hep-ph/9707435. [Adv. Ser. Direct. High Energy Phys.21,565(2010)].
- [73] Probir Roy. Supersymmetric theories with explicit R-parity violation. In *Pacific particle physics phenomenology. Proceedings, APCTP Workshop, Seoul, Korea, October 31-November 2, 1997*, pages 10–17, 1997, hep-ph/9712520.
- [74] Rabindra N. Mohapatra. Supersymmetry and R-parity: an Overview. *Phys. Scripta*, 90:088004, 2015, 1503.06478.
- [75] Florian Staub. SARAH. <https://sarah.hepforge.org/trac/wiki/MSSM-RpV-LnV>.
- [76] Sourov Roy and Biswarup Mukhopadhyaya. Some implications of a supersymmetric model with R-parity breaking bilinear interactions. *Phys. Rev.*, D55:7020–7029, 1997, hep-ph/9612447.
- [77] Marco A. Diaz, Jorge C. Romao, and J. W. F. Valle. Minimal supergravity with R-parity breaking. *Nucl. Phys.*, B524:23–40, 1998, hep-ph/9706315.
- [78] Chao-hsi Chang and Tai-fu Feng. The Minimum supersymmetric standard model without lepton numbers and R-parity. 1999, hep-ph/9908295.
- [79] Biswarup Mukhopadhyaya and Sourov Roy. Radiative decay of the lightest neutralino in an R-parity violating supersymmetric theory. *Phys. Rev.*, D60:115012, 1999, hep-ph/9903418.
- [80] Sacha Davidson, Marta Losada, and Nuria Rius. Neutral Higgs sector of the MSSM without R(p). *Nucl. Phys.*, B587:118–146, 2000, hep-ph/9911317.
- [81] Javier Ferrandis. Basis independent study of supersymmetry without R-parity and the tau-neutrino mass. *Phys. Rev.*, D60:095012, 1999, hep-ph/9810371.
- [82] Sacha Davidson and Marta Losada. Basis independent neutrino masses in the R(p) violating MSSM. *Phys. Rev.*, D65:075025, 2002, hep-ph/0010325.
- [83] Yuval Grossman and Howard E. Haber. Basis independent analysis of the sneutrino sector in R-parity violating supersymmetry. *Phys. Rev.*, D63:075011, 2001, hep-ph/0005276.
- [84] Florian Staub. Exploring new models in all detail with SARAH. *Adv. High Energy Phys.*, 2015:840780, 2015, 1503.04200.
- [85] Florian Staub, Thorsten Ohl, Werner Porod, and Christian Speckner. A Tool Box for Implementing Supersymmetric Models. *Comput. Phys. Commun.*, 183:2165–2206, 2012, 1109.5147.
- [86] Florian Staub. SARAH 4 : A tool for (not only SUSY) model builders. *Comput. Phys. Commun.*, 185:1773–1790, 2014, 1309.7223.
- [87] Florian Staub. SARAH. <https://sarah.hepforge.org/trac/wiki/MSSM-RpV-Bi>.
- [88] S Heinemeyer, Wolfgang F L Hollik, and Georg Weiglein. FeynHiggsFast: a program for a fast calculation of masses and mixing angles in the Higgs Sector of the MSSM. Technical Report hep-ph/0002213. CERN-TH-2000-055. DESY-2000-020. KA-TP-2000-3. DESY-00-020, CERN, Geneva, Feb 2000.
- [89] Howard E. Haber. Challenges for nonminimal Higgs searches at future colliders. In *Perspectives for electroweak interactions in e+ e- collisions. Proceedings, Ringberg Workshop, Tegernsee, Germany, February 5-8, 1995*, pages 219–232, 1996, hep-ph/9505240. [,151(1995)].
- [90] Marcela Carena and Howard E. Haber. Higgs Boson Theory and Phenomenology. *Prog. Part. Nucl. Phys.*, 50:63–152, 2003, hep-ph/0208209.
- [91] Wei-Shu Hou, Rishabh Jain, Chung Kao, Masaya Kohda, Brent McCoy, and Amarjit Soni. Flavor Changing Heavy Higgs Interactions with Leptons at Hadron Colliders. 2019, 1901.10498.
- [92] Kingman Cheung, Jae Sik Lee, and Po-Yan Tseng. New Emerging Results in Higgs Precision Analysis Updates 2018 after Establishment of Third-Generation Yukawa Couplings. 2018, 1810.02521.
- [93] Peter Athron et al. Combined collider constraints on neutralinos and charginos. *Eur. Phys. J.*, C79(5):395, 2019, 1809.02097.
- [94] Ulrich Haisch and Farvah Mahmoudi. MSSM: Cornered and Correlated. *JHEP*, 01:061, 2013, 1210.7806.
- [95] B. C. Allanach, A. Dedes, and Herbert K. Dreiner. Bounds on R-parity violating couplings at the weak scale and at the GUT scale. *Phys. Rev.*, D60:075014, 1999, hep-ph/9906209.
- [96] Otto C. W. Kong and Rishikesh D. Vaidya. Radiative B decays in supersymmetry without R-parity. *Phys. Rev.*, D71:055003, 2005, hep-ph/0403148.
- [97] Otto C. W. Kong and Rishikesh D. Vaidya. Some novel contributions to radiative B decay in supersymmetry without R-parity. *Phys. Rev.*, D72:014008, 2005, hep-ph/0408115.

- [98] Otto C. W. Kong and Rishikesh Vaidya. tan beta enhanced contributions to $b \rightarrow s + \gamma$ in SUSY without R-parity. In *Supersymmetry and unification of fundamental interactions. Proceedings, 12th International Conference, SUSY 2004, Tsukuba, Japan, June 17-23, 2004*, pages 661–664, 2004, hep-ph/0411165.
- [99] Rishikesh D. Vaidya and Otto C. W. Kong. $B \rightarrow X(s) + \gamma$ in supersymmetry without R-parity. *J. Korean Phys. Soc.*, 45:S417–S423, 2004, hep-ph/0411336. [383(2004)].
- [100] King-man Cheung and Otto C. W. Kong. Muon $\rightarrow e \gamma$ from supersymmetry without R-parity. *Phys. Rev.*, D64:095007, 2001, hep-ph/0101347.
- [101] Chien-Yi Chen and Otto C. W. Kong. Leptonic Radiative Decay in Supersymmetry without R parity. *Phys. Rev.*, D79:115013, 2009, 0901.3371.
- [102] Chan-Chi Chiou, Otto C. W. Kong, and Rishikesh D. Vaidya. Quark Loop Contributions to Neutron, Deuteron, and Mercury EDMs from Supersymmetry without R parity. *Phys. Rev.*, D76:013003, 2007, 0705.3939.
- [103] Y. Y. Keum and Otto C. W. Kong. R-parity violating contribution to neutron EDM at one loop. *Phys. Rev. Lett.*, 86:393–396, 2001, hep-ph/0004110.
- [104] Darwin Chang, We-Fu Chang, Mariana Frank, and Wai-Yee Keung. The Neutron electric dipole moment and CP violating couplings in the supersymmetric standard model without R-parity. *Phys. Rev.*, D62:095002, 2000, hep-ph/0004170.
- [105] Nodoka Yamanaka, Toru Sato, and Takahiro Kubota. A Reappraisal of two-loop contributions to the fermion electric dipole moments in R-parity violating supersymmetric models. *Phys. Rev.*, D85:117701, 2012, 1202.0106.
- [106] Nodoka Yamanaka, Toru Sato, and Takahiro Kubota. Linear programming analysis of the R-parity violation within EDM-constraints. *JHEP*, 12:110, 2014, 1406.3713.
- [107] Kota Yanase, Naotaka Yoshinaga, Koji Higashiyama, and Nodoka Yamanaka. Electric dipole moment of ^{199}Hg atom from P , CP -odd electron-nucleon interaction. *Phys. Rev.*, D99(7):075021, 2019, 1805.00419.
- [108] Saurabh Bansal, Antonio Delgado, Christopher Kolda, and Mariano Quiros. Limits on R-parity-violating couplings from Drell-Yan processes at the LHC. 2018, 1812.04232.
- [109] M. Tanabashi et al. Review of Particle Physics. *Phys. Rev.*, D98(3):030001, 2018.
- [110] J. Lesgourgues and L. Verde. Neutrinos in Cosmology. *Phys. Rev.*, D98(3):030001, 2018.
- [111] J. Schechter and J. W. F. Valle. Neutrino Decay and Spontaneous Violation of Lepton Number. *Phys. Rev.*, D25:774, 1982.
- [112] J. W. F. Valle. Fast Neutrino Decay in Horizontal Majoron Models. *Phys. Lett.*, 131B:87, 1983.
- [113] G. B. Gelmini and J. W. F. Valle. Fast Invisible Neutrino Decays. *Phys. Lett.*, 142B:181–187, 1984.
- [114] M. C. Gonzalez-Garcia and J. W. F. Valle. Fast Decaying Neutrinos and Observable Flavor Violation in a New Class of Majoron Models. *Phys. Lett.*, B216:360–366, 1989.
- [115] Anjan S. Joshipura and Saurabh D. Rindani. Fast neutrino decay in the minimal seesaw model. *Phys. Rev.*, D46:3000–3007, 1992, hep-ph/9205220.
- [116] A. D. Dolgov, S. Pastor, J. C. Romao, and J. W. F. Valle. Primordial nucleosynthesis, Majorons and heavy tau neutrinos. *Nucl. Phys.*, B496:24–40, 1997, hep-ph/9610507.
- [117] Miguel Escudero and Malcolm Fairbairn. Cosmological Constraints on Invisible Neutrino Decays Revisited. 2019, 1907.05425.
- [118] Y. Chikashige, Rabindra N. Mohapatra, and R. D. Peccei. Spontaneously Broken Lepton Number and Cosmological Constraints on the Neutrino Mass Spectrum. *Phys. Rev. Lett.*, 45:1926, 1980. [921(1980)].
- [119] J. W. F. Valle. Gauge theories and the physics of neutrino mass. *Prog. Part. Nucl. Phys.*, 26:91–171, 1991.
- [120] J. C. Romao. Phenomenology of supersymmetric theories with and without R parity. *Nucl. Phys. Proc. Suppl.*, 95:243–251, 2001, hep-ph/0011378. [243(2000)].
- [121] John F. Beacom and Nicole F. Bell. Do solar neutrinos decay? *Phys. Rev. D*, 65:113009, Jun 2002.
- [122] R. Picoreti, M. M. Guzzo, P. C. de Holanda, and O. L. G. Peres. Neutrino Decay and Solar Neutrino Seasonal Effect. *Phys. Lett.*, B761:70–73, 2016, 1506.08158.
- [123] B. Aharmim et al. Constraints on Neutrino Lifetime from the Sudbury Neutrino Observatory. *Phys. Rev.*, D99(3):032013, 2019, 1812.01088.
- [124] Jeffrey M. Berryman, André de Gouvêa, and Daniel Hernández. Solar neutrinos and the decaying neutrino hypothesis. *Phys. Rev. D*, 92:073003, Oct 2015.
- [125] Lena Funcke, Georg Raffelt, and Edoardo Vitagliano. Distinguishing Dirac and Majorana neutrinos by their gravi-majoron decays. 2019, 1905.01264.
- [126] M. C. Gonzalez-Garcia and M. Maltoni. Status of Oscillation plus Decay of Atmospheric and Long-Baseline Neutrinos. *Phys. Lett.*, B663:405–409, 2008, 0802.3699.
- [127] R. A. Gomes, A. L. G. Gomes, and O. L. G. Peres. Constraints on neutrino decay lifetime using long-baseline charged and neutral current data. *Phys. Lett.*, B740:345–352, 2015, 1407.5640.
- [128] Sandhya Choubey, Debajyoti Dutta, and Dipyaman Pramanik. Invisible neutrino decay in the light of NOvA and T2K data. *JHEP*, 08:141, 2018, 1805.01848.
- [129] John F. Beacom, Nicole F. Bell, and Scott Dodelson. Neutrinoless universe. *Phys. Rev. Lett.*, 93:121302, 2004, astro-ph/0404585.
- [130] Maria Archidiacono, Steen Hannestad, Rasmus Sloth Hansen, and Thomas Tram. Cosmology with self-interacting sterile neutrinos and dark matter - A pseudoscalar model. *Phys. Rev.*, D91(6):065021, 2015, 1404.5915.
- [131] Christina D. Kreisch, Francis-Yan Cyr-Racine, and Olivier DorÁf. The Neutrino Puzzle: Anomalies, Interactions, and Cosmological Tensions. 2019, 1902.00534.
- [132] Yasaman Farzan. Ultra-light scalar saving the 3+1 neutrino scheme from the cosmological bounds. 2019, 1907.04271.

- [133] J. D. Vergados. Neutrinoless Double Beta Decay Without Majorana Neutrinos in Supersymmetric Theories. *Phys. Lett.*, B184:55–62, 1987.
- [134] M. Hirsch, H. V. Klapdor-Kleingrothaus, and S. G. Kovalenko. Supersymmetry and neutrinoless double beta decay. *Phys. Rev.*, D53:1329–1348, 1996, hep-ph/9502385. [,787(1995)].
- [135] G. Abbiendi et al. Search for nearly mass degenerate charginos and neutralinos at LEP. *Eur. Phys. J.*, C29:479–489, 2003, hep-ex/0210043.
- [136] Biswarup Mukhopadhyaya. Supersymmetry and neutrino mass. *Proc. Indian Natl. Sci. Acad.*, A70(1):239–249, 2004, hep-ph/0301278.
- [137] Sebastian Dumitru, Burt A. Ovrut, and Austin Purves. The R -parity Violating Decays of Charginos and Neutralinos in the B-L MSSM. *JHEP*, 02:124, 2019, 1810.11035.
- [138] Giovanna Cottin, Marco Aurelio Diaz, Sebastian Olivares, and Nicolas Rojas. Implications of Bilinear R-Parity Violation on Neutrinos and Lightest Neutralino Decay in Split Supersymmetry. 2012, 1211.1000.
- [139] F. de Campos, M. A. Diaz, O. J. P. Eboli, M. B. Magro, W. Porod, and S. Skadhauge. CERN LHC signals for neutrino mass model in bilinear R-parity violating mAMSB. *Phys. Rev.*, D77:115025, 2008, 0803.4405.
- [140] A. Djouadi, Y. Mambrini, and M. Muhlleitner. Chargino and neutralino decays revisited. *Eur. Phys. J.*, C20:563–584, 2001, hep-ph/0104115.
- [141] Shaouly Bar-Shalom and Amarjit Soni. Universally enhanced light-quarks Yukawa couplings paradigm. *Phys. Rev.*, D98(5):055001, 2018, 1804.02400.
- [142] Charalampos Anastasiou, Claude Duhr, Falko Dulat, Elisabetta Furlan, Thomas Gehrmann, Franz Herzog, Achilleas Lazopoulos, and Bernhard Mistlberger. High precision determination of the gluon fusion Higgs boson cross-section at the LHC. *JHEP*, 05:058, 2016, 1602.00695.
- [143] Robert V. Harlander. Higgs production in heavy quark annihilation through next-to-next-to-leading order QCD. *Eur. Phys. J.*, C76(5):252, 2016, 1512.04901.
- [144] Miguel Crispim Romão, Athanasios Karozas, Stephen F. King, George K. Leontaris, and Andrew K. Meadowcroft. R-Parity violation in F-Theory. *JHEP*, 11:081, 2016, 1608.04746.
- [145] J. Alwall, R. Frederix, S. Frixione, V. Hirschi, F. Maltoni, O. Mattelaer, H. S. Shao, T. Stelzer, P. Torrielli, and M. Zaro. The automated computation of tree-level and next-to-leading order differential cross sections, and their matching to parton shower simulations. *JHEP*, 07:079, 2014, 1405.0301.
- [146] M. Tanabashi et al. Review of Particle Physics. *Phys. Rev.*, D98(3):030001, 2018.
- [147] Jihn E. Kim, Bumseok Kyae, and Hyun Min Lee. Effective supersymmetric theory and $(g-2)$ (muon with R-parity violation). *Phys. Lett.*, B520:298–306, 2001, hep-ph/0103054.
- [148] Abdelhak Djouadi. The Anatomy of electro-weak symmetry breaking. I: The Higgs boson in the standard model. *Phys. Rept.*, 457:1–216, 2008, hep-ph/0503172.